



School of Mechanical and Manufacturing Engineering

Faculty of Engineering

UNSW Sydney

BY

Chi Shen

**Impact of Curvature, Bifurcation and Stenting on Secondary Flow in
Idealised and Realistic Coronary Arteries**

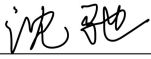
Thesis submitted as a requirement for the degree of Master in
Mechanical Engineering

Submitted: 8/7/2020
Supervisor: Susann Beier (UNSW)

Student zID: z5194825

ORIGINALITY STATEMENT

'I hereby declare that this submission is my own work and to the best of my knowledge it contains no materials previously published or written by another person, or substantial proportions of material which have been accepted for the award of any other degree or diploma at UNSW or any other educational institution, except where due acknowledgement is made in the thesis. Any contribution made to the research by others, with whom I have worked at UNSW or elsewhere, is explicitly acknowledged in the thesis. I also declare that the intellectual content of this thesis is the product of my own work, except to the extent that assistance from others in the project's design and conception or in style, presentation and linguistic expression is acknowledged.'

Signed 

Date 8 / 7 / 2020

Abstract

The objective of this study is to generate insights into the effect of curved small-scale bifurcations with and without stents on secondary flow profiles and resulting WSS and TAWSS effects. The influence of curvature in bifurcating vessels leads to the skew, spin, asymmetry of the Dean-like flow. The secondary flow structures result in low TAWSS regions promoting plaque deposition. The presence of stents can dissipate vortices in the daughter branches as well in stented configurations. Overall, this new knowledge contributes to a better understanding of the effect of small vessel geometry on flow patterns and their effects on local TAWSS.

Acknowledgements

I am highly indebted to Susann Beier for guidance and constant supervision as well as for providing valuable detailed feedback. I will express my appreciation to Ramtin Gharleghi for all his help on the questions I asked. Thank Somesh Khullar for his help on application of NCI and KATANA as well as Vanessa Luvio for the information of commercial stent design. The simulations in this work was undertaken with the assistance of resources from the National Computational Infrastructure (NCI), an NCRIS enabled facility supported by the Australian Government, and KATANA (UNSW)

Contents

Abstract.....	iii
Acknowledgements.....	iv
List of Figures.....	vii
List of Tables	ix
Nomenclature.....	x
1. Introduction.....	1
2. Literature review	4
3. Methodology	7
3.1 Geometries	7
3.1.1 Definition of ideal cylinder vessels.....	7
3.1.2 Definition of ideal vessels with bifurcation	7
3.1.3 Patient-specific geometries	8
3.1.4 Stented geometries	9
3.2 Computational Fluid Dynamics Analysis	12
4. Results.....	13
4.1 Secondary flow	13
4.1.1 The influence of curvature on secondary flow.....	13
4.1.2 The influence of bifurcation angle on secondary flow.....	18
4.1.3 The influence of stent on secondary flow	18
4.2 WSS	19
4.2.1 The influence of curvature on WSS	19
4.2.2 The influence of bifurcation angle on WSS.....	20
4.2.3 The influence of stent on WSS	21
4.3 TAWSS.....	26
4.3.1 The influence of curvature on TAWSS.....	26

4.3.2 The influence of bifurcation angle on TAWSS.....	27
4.3.3 The influence of stents on TAWSS.....	29
5. Discussion.....	32
6. Conclusion	33
References.....	34
Appendix.....	36

List of Figures

Figure 1 The progression of atherosclerosis [5]	1
Figure 2 Stent in coronary artery [14].....	2
Figure 3 LowWSS region exists in large BA models [19]	4
Figure 4 Correlation between tortuosity and Low WSS [20]	5
Figure 5 Symmetry loss due to side branch	5
Figure 6 Definition of curvature	7
Figure 7 Definition of ideal bifurcation.....	8
Figure 8 Centerline generation in VMTK [31].....	9
Figure 9 Stent 1 with rectangle cross-section	9
Figure 10 Stent 2 with circular cross-section.....	9
Figure 11 Generation of thick stent wall	10
Figure 12 Generation of connectors.....	10
Figure 13 generation of stent ring	11
Figure 14 Substraction of stent	11
Figure 15 Face inflaction (left) and edge size (right)	12
Figure 16 Cross-section planes defined in bifurcation models	13
Figure 18 Dean-like flow in 5 cross-section planes of 105° ideal cylinder models	14
Figure 17 Dean-like flow in in ideal cylinder models with differernt curvature	14
Figure 19 Dean-like flow in proximal MB (S1).....	15
Figure 20 Dean-like flow in divider region (S2).....	15
Figure 21 Velocity contour of S3 and Dean-like flow in distal MB(S3, S4) of non-stented bifurcations ...	16
Figure 23 Dean-like flow in distal MB of 48° curved non-stented models with 38°, 68°, 98°, 128° BA ...	17

Figure 22 Velocity contour of S3 and Dean-like flow in SB (S5, S6) of ideal non-stented bifurcations with different curvature (0°, 45°, 75°, 105)° and 105° curved patient-specific model..	17
Figure 24 Comparision of non-stented and stented 105° curvved models with 68° BA	18
Figure 25 WSS distributions of 0°, 45°, 75°, 105°curved patient-specific bifurcation with fixed BA (68°) in front, back, left, right view and contours of adverse WSS	19
Figure 26 WSS distributions of 0°, 45°, 75°, 105°curved patient-specific bifurcation with fixed BA (68°) in bottome view	20
Figure 27 WSS distributions of 45°curved patient-specific bifurcation with 38°, 68°, 98°, 128° BA in front, back, left, right view and contours of adverse WSS	20
Figure 28 WSS distributions of 45°curved patient-specific bifurcation with 38°, 68°, 98°, 128° BA in bottom view	21
Figure 29 WSS distributions of 45°curved patient-specific bifurcation with 38°, 68°, 98°, 128° BA in front, left, right, bottom view and contours of adverse WSS	21
Figure 30 Percentage of low WSS area of non-stented patient-specific bifurcations	22
Figure 31 Percentage of low WSS area of patient-specific bifurcations with stent 1	23
Figure 32 Percentage of low WSS area of patient-specific bifurcations with stent 2	23
Figure 34 Percentage of high WSS area of patient-specific bifurcations with stent 1	24
Figure 33 Percentage of high WSS area of non-stented patient-specific bifurcations	24
Figure 35 Percentage of high WSS area of patient-specific bifurcations with stent 2	25
Figure 36 TAWSS distributions of 0°, 45°, 75°, 105°curved patient-specific bifurcation with fixed BA (68°) in front, back view and contours of adverse WSS	26
Figure 37 TAWSS distributions of 45°curved patient-specific bifurcation with 38°, 68°, 98°, 128° BA in front, back, left, right view and contours of adverse WSS	28
Figure 38 TAWSS distributions of 45°curved patient-specific bifurcation with 38°, 68°, 98°, 128° BA in bottom view	28
Figure 39 TAWSS distributions of 45°curved patient-specific bifurcation with 38°, 68°, 98°, 128° BA in front, left, right, bottom view and contours of adverse WSS	29
Figure 41 Percentage of low TAWSS area of patient-specific bifurcations with stent1	30
Figure 40 Percentage of low TAWSS area of non-stented patient-specific bifurcations	30
Figure 42 Percentage of low TAWSS area of patient-specific bifurcations with stent2	31

List of Tables

Table 1 Geometried simulated in this project6

Nomenclature

θ	= Central angle
k	= Curvature
l	= Length of curved segment
R	= Radius

1. Introduction

Atherosclerotic cardiovascular disease (ASCVD) is one of the main causes of death around the world [1]. According to World Health Organization (WHO), the deaths due to coronary artery disease (CAD) will rise to 11 million by 2020, which is over 1.5 times than the death number in 2002 (7 million) [2]. Coronary Atherosclerosis is formed when the coronary arteries are narrowed by the fatty deposits which is clinically called plaques [3]. The coronary arteries are the important role to deliver blood to the heart. Occlusion of the coronary leads to myocardial ischemia which upsets the balance the oxygen supply and the heart tissue demand [4]. Once the occlusion lasts a long period, the potential of myocardial infarction rise, which is seriously dangerous can cause a sudden death [1].

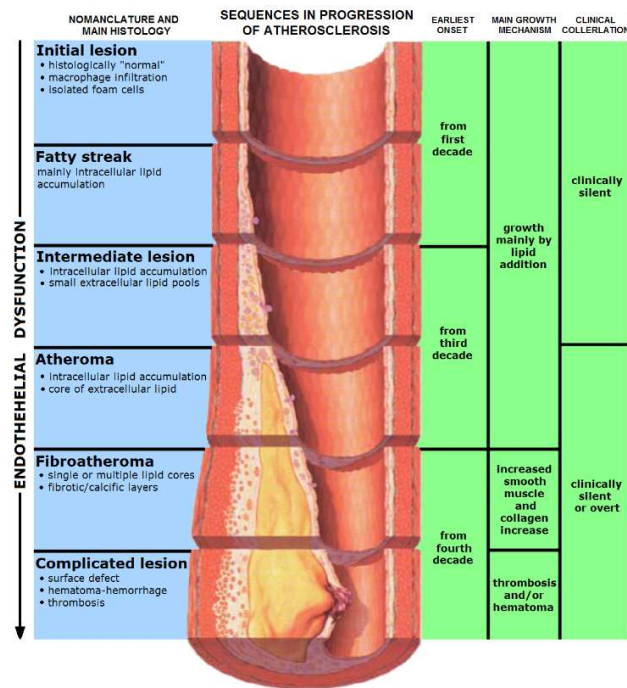


Figure 1 The progression of atherosclerosis [5]

It is generally believed that the occurrence and development of atherosclerosis are related to the complex flow field in curvature and bifurcating area of the large and medium arteries [6, 7]. In order to understand the relationship between vascular morphology and atherosclerosis, numerous clinical, numerical studies based on rigid idealized models and actual geometric models have been conducted.

Wahle et al [8]. demonstrated by means of X-ray angiography and intravascular ultrasound that the distribution of plaque was determined by the local curvature of most blood vessels. In most vessels, the

plaque developed more often in inner surface of curvature than in outer surface of curvature. The low wall shear stress associated with the inner surface of vessel curvature may lead to the initial formation of atherosclerotic plaques in human coronary arteries. This is also proved by O. Smedby et al. [9] who adopted digitized angiography and edge-roughness calculations to study the atherosclerosis development in 301 hyperlipidemic patients. The explanation for more often plaque development in inner curvature from authors was that the flow disturbances such as low shear rate and flow separation tended to develop along the inner curvature and thus, promoted the development of atherosclerosis.

Because of the high mortality rates [10], researches have been carried out to cut mortality down to an acceptable level. Long-term studies have confirmed that hemodynamics is the key to solving the current dilemma in CAD [11]. By virtue of blood flow viscosity, a frictional force per unit area, which is termed as wall shear stress (WSS), exists on the endothelial surface and arterial vessel wall. Pathologically, the formation of atherosclerosis is a complex multifaceted process, however, WSS, TAWSS has been recognized as an essential inducement of ISR and ST. Generally, adverse WSS and TAWSS range is: Low WSS < 0.5 Pa, high WSS > 2.5 Pa and low TAWSS < 0.5 Pa.

Percutaneous coronary intervention (PCI) with stent is the most pervasive treatment for atherosclerotic cardiovascular disease [12]. PCI essentially is percutaneous coronary lumen enlargement technique [13] used to widen vessel diameter and help blood transfer to body issues.

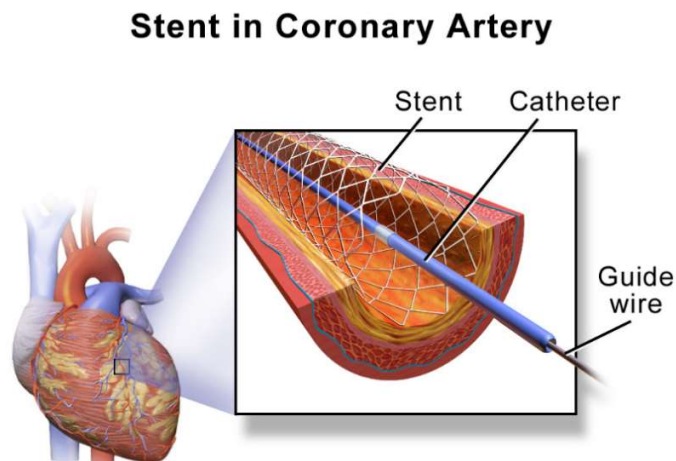


Figure 2 Stent in coronary artery [14]

Benefiting from computational fluid dynamics (CFD) method, deep research has been conducted on the vessel structure and stent design to achieve better understanding on the hemodynamics. Research has

indicated that atherogenesis preferentially forms near arterial bifurcations and curvatures [15-17], however, the influence of curvature and bifurcation is still not clear enough. The flow patterns such as velocity, secondary flow are discovered to have direct influence on local WSS distribution which result in cardiovascular disease. However, the relationship of vessel structure, secondary flow and hemodynamics is still not clear. Besides, most previous researches did not combine the influence of implanted stents and complex vessel structure together.

In this project, ideal cylinder models, ideal bifurcation models and patient-specific models are adopted to investigate and two types of stents are implanted to investigate the relationship between secondary flow and vessel structure, implants. CFD method is adopted to simulate hemodynamics in these models.

2. Literature review

Sun et al. [18] used multi-slice CT angiography to study the relationship between left coronary artery bifurcation and coronary artery lesion. CT angiography was performed on 30 patients with suspected coronary artery disease 89% of whom had plaque bifurcation angles greater than 90 degrees. This study showed a direct link between bifurcation angle and plaque formation, which was also proved by many previous study. Therefore, different bifurcation angles have been studied numerically.

T. Chaichana et al. [19] conducted a computational fluid dynamics (CFD) analysis using eight ideal models with different bifurcation angles (15°, 30°, 45°, 60°, 75°, 90°, 105° and 120°) and four ideal models (narrow angles of 58° and 73°, wide angles of 110° and 120°) to simulate realistic hemodynamics in human vascular. The results showed that a wide range of WSS area was found in the model with larger bifurcation angles (Figure 3), and the wall pressure decreases when the flow from the left trunk to the bifurcation region changes.

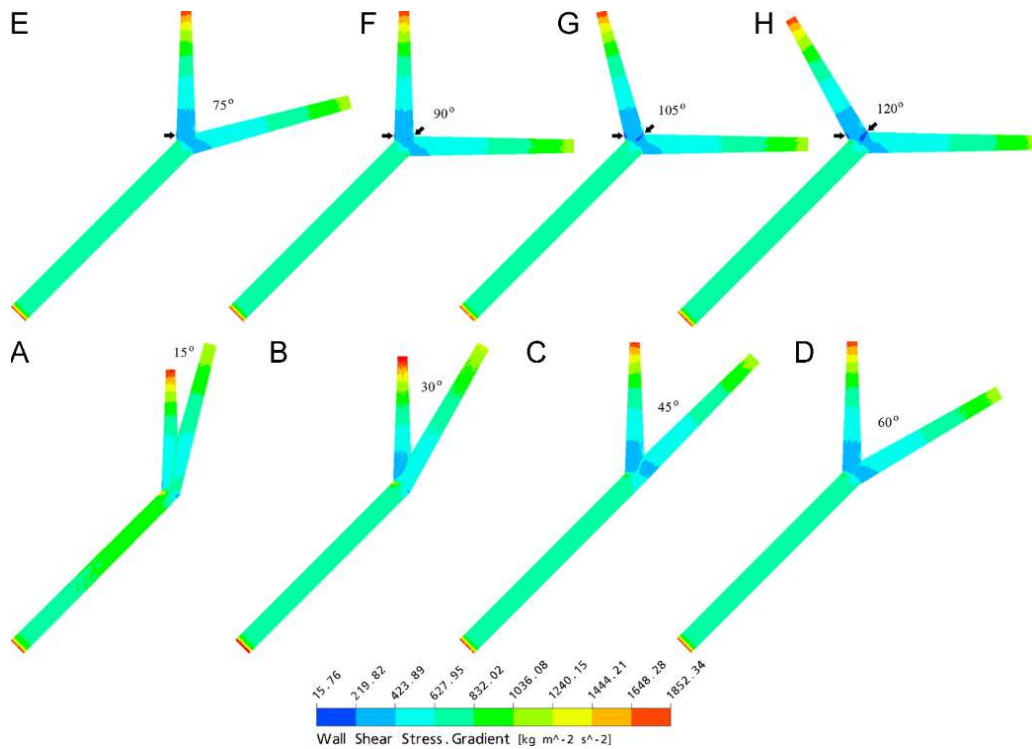


Figure 3 LowWSS region exists in large BA models [19]

However, M. Malvè et al. [20] introduced new opinion about the relationship between atherosclerosis and bifurcation geometric factors. Low WSS region was found in outer surface of daughter branches. The result

showed that the tortuosity was an emergent geometric factor to determine low WSS in outer surface of daughter branches other than bifurcation angles which showed apparent relationship with high WSS region.

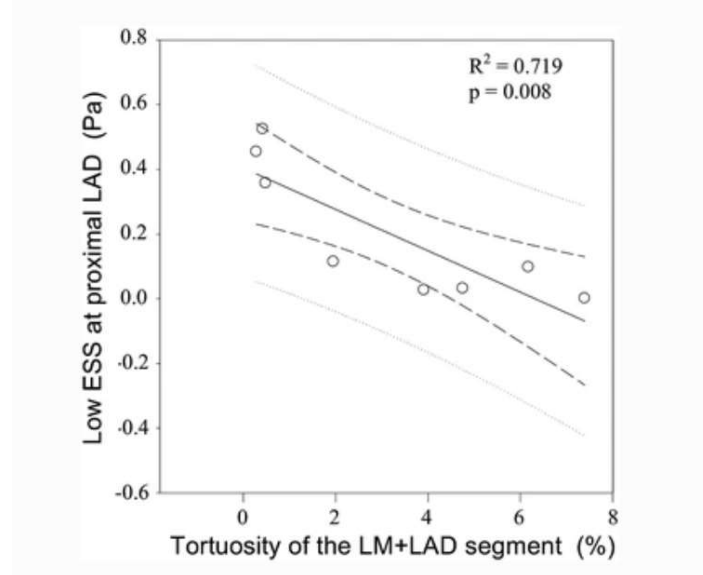


Figure 4 Correlation between tortuosity and Low WSS [20]

Regions of bifurcation and strong curvature develop Dean-like secondary flow and are prone to atherosclerosis development. Dean first investigated vessel curvature and its effect on flow dynamics in pipes [21], in which secondary flow moved from the outer to the inner surfaces in the middle of a curved pipe, which has been studied in coronary arteries as well [2]. In bifurcating vessels, the velocity skews towards the divider [22], and the Dean-like flow loses its symmetry due to the presence of the side branch [23], with the bifurcation dominating the flow velocity profiles in the distal daughter branches [24].

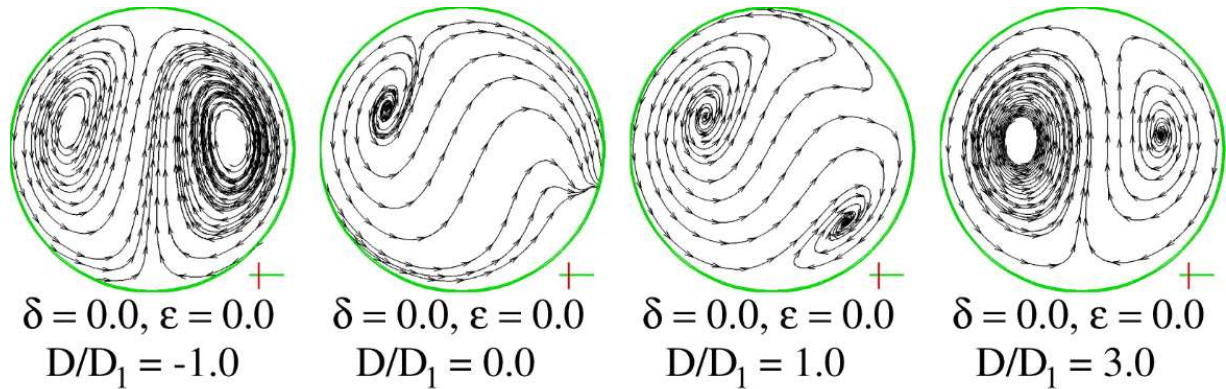


Figure 5 Symmetry loss due to side branch

The curvature of the artery was found to have a neglectable influence on the flow physics initially increasing as it moves downstream, with distance to the bifurcation region [25]. Studies have also reported that the curvature leads to asymmetric velocity streamlines and a strong vortex gradually dominating the secondary flow field in the daughter branches [26, 27]. Additionally, the rheological properties of blood also influenced the local hemodynamics. It was found that the Newtonian fluid was more sensitive to the vessel structure such as curvature, while non-Newtonian blood led to less velocity fluctuation and negligible rotation of flow velocity profiles [26].

Previous work has been mainly using idealised models [28, 29] There has been no previous investigations on the effects of curvature, bifurcation and the presence of stents to compare their effects. Further, there is currently no clear understanding of the skew of Dean-like flow and its direction in relation to curvatures in a bifurcation. Here, the side branch and curvature were judged separately as a potential cause of velocity profile skewing. The influence of the presence of stents on secondary flow is an important factor in post-surgical care and there has been little work done on this aspect in the context of WSS development and restenosis. Therefore, here the influence of curvature, bifurcation, and stents on the secondary flow in vessels is studied using an ideal cylinder, idealised bifurcation models with a range of curvatures (0° , 45° , 75° , 105°) and a range of bifurcation angles (38° , 68° , 98° , 128°). The geometry parameters are determined based on patient-specific models. In addition, patient-specific bifurcations with similar curvature and bifurcation angles) are also analysed to study their implications on real-life scenarios. All the models are also stented with a rectangular cross-section stent and a commercial stent (Onyx type by *Medtronic*) to investigate the influence of stents. Overall, this work may increase understanding of secondary flow fields in bifurcating coronaries associated with atherosclerosis development.

Table 1 Geometries simulated in this project

	Curvature ($0^\circ, 45^\circ, 75^\circ, 105^\circ$)			Bifurcation angles ($38^\circ, 68^\circ, 98^\circ, 128^\circ$)		
Type	Non-stented	Stent 1	Stent 2	Non-stented	Stent 1	Stent 2
Ideal cylinder	4	4	4	N/A	N/A	N/A
Ideal bifurcation	4	4	4	12	12	12
Patient specific bifurcation	4	4	4	12	12	12
Total	108					

3. Methodology

3.1 Geometries

3.1.1 Definition of ideal cylinder vessels

The straight vessel is set to be a rigid cylinder pipe with a diameter of 3 mm, a common diameter of coronary artery in the adult which has been already confirmed by a echocardiographic visualization research of Douglas et al [30]. The length of the stented section of cylinder vessel is assumed to be 10 mm, and there are 6-mm-long sections without stent on the both sides of the stented section. Thus, the total length of the straight vessel is 22 mm.

The centerline of the curved cylindrical model is defined as an arc (Figure 6) with the diameter and length of curved segment being 3mm and 10mm, respectively. These are estimated using the equations: $k = \frac{1}{R}$, $l = R \cdot \theta$, $k = \frac{\theta}{l}$ ($k = \text{curvature}$, $R = \text{radius}$, $\theta = \text{central angle}$), with a central angle defining the curvature. Since the curved segment is of fixed length, a larger central angle represents a larger curvature. Thus, the curved cylinder models are set to 45°, 75° and 105° curvature magnitudes.

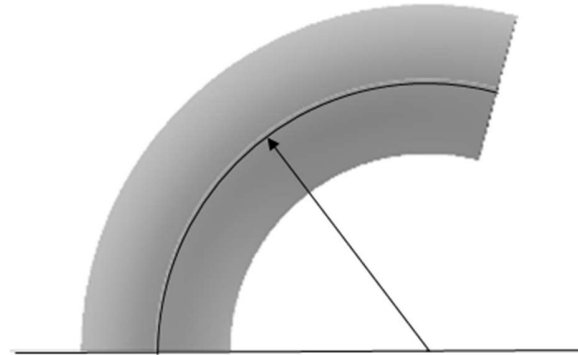


Figure 6 Definition of curvature

3.1.2 Definition of ideal vessels with bifurcation

The ideal bifurcation is defined to wrap around a sphere which simulates the heart (Figure 7.). The curvature of the main branch (MB) and side branch (SB) are determined by the central angle in the same manner as the ideal cylinder model. Parameters of the ideal bifurcation model are determined based off a patient-specific bifurcation geometry with the length and diameter of MB and SB are 27.5 mm and 11 mm, and the diameters, 2.8 mm, and 2 mm, respectively and a bifurcation angle of 38°, 68°, 98°, 128°.



Figure 7 Definition of ideal bifurcation

3.1.3 Patient-specific geometries

In this thesis, a patient-specific geometry will be used to simulate blood flow in real body vessels. The .stl file is a 3D mesh geometry file which is only a surface geometry consists of mesh elements. To generate model of vessels of bifurcation for further processing, the mesh geometry should be converted to a solid body.

Although the solid body can be generated, there is no basis for CAD operations. A centerline is generated by using VMTK. Centerlines are important and necessary information for geometry modelling. VMTK is an open source software using Python to realize powerful operation on the vessel geometries. As shown in Figure 8, centerline can be generated directly in VMTK by using Voronoi diagram method which is packaged in VMTK. To obtain patient-specific models with the same curvatures of ideal models. The initial patient-specific model is modified in Solidworks.

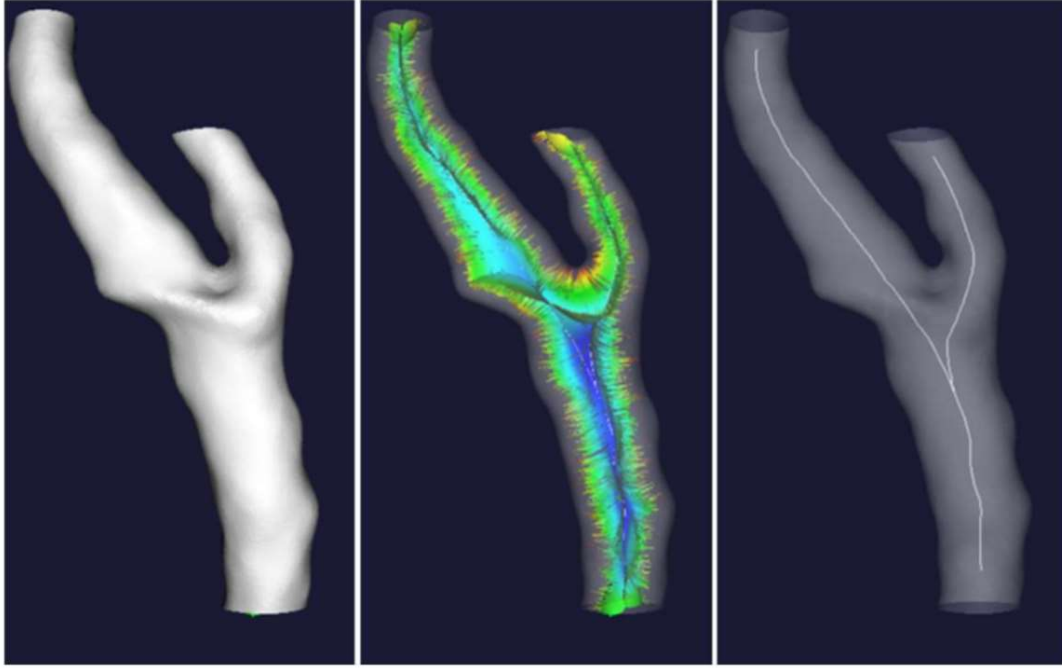


Figure 8 Centerline generation in VMTK [31]

3.1.4 Stented geometries

Two kind of stents are adopted in this project. Stent 1 (Figure 9) is an ideal model with rectangle cross-section (0.07 mm each side) and spline shape connectors. Stent 2 (Figure 10) is a commercial stent (Onyx by Medtronic) with a circular cross-section (radius=0.081 mm) and straight connectors.

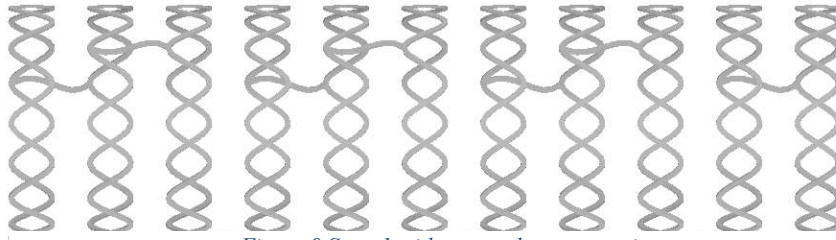


Figure 9 Stent 1 with rectangle cross-section

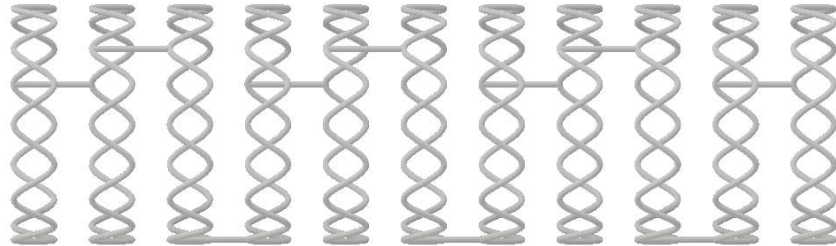


Figure 10 Stent 2 with circular cross-section

As the vessels are curved or with bifurcation, the regular method that uses single Boolean Function step to generate blood flow cannot work. Distortion happens on the interface between stents and curved blood flow, especially in the connectors area. Inspired by the method shown in the research of J. GUNDERT et al [32], a new method is developed to model the geometries of stents and blood flow. Taking the stent geometry of the curved vessel (105°) as an example, figure 11 illustrates the process to generate an optimized blood flow. To improve the accuracy of geometries, as shown in Figure 11, the stent geometry is modified into a thick stent to yield an accurate stent geometry which fits the vessels.

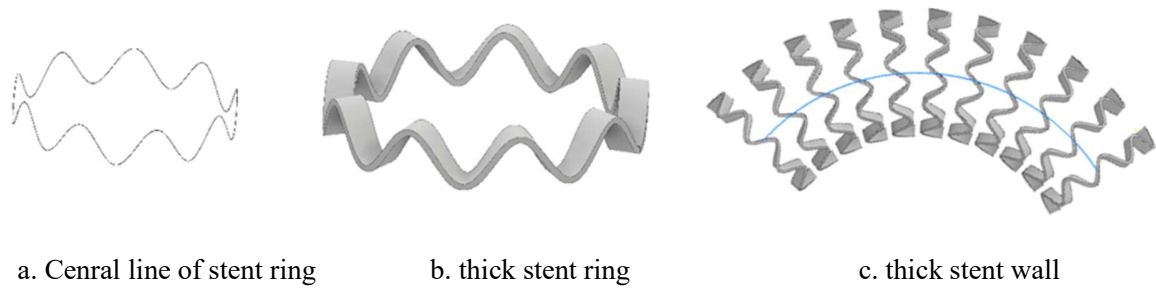


Figure 11 Generation of thick stent wall

It is a challenge to model the connectors as the entire connectors should follow the curvature in curved vessels and the change of the diameters in patient-specific vessel geometry. To overcome this barrier, a guide surface which has the same diameter of the vessels should be generated. A 2D spline shape curve line is generated on the plane which is across both connect points on the two adjacent stent rings. And this plane should be parallel to another plane that is tangent to the guide cylinder surface. Then, the 2D curve line is projected to the cylinder surface (Figure 12.a), which makes the connector geometry fits the curvature accurately (Figure 12.b). Figure 12.c shows the entire thick stent geometry of the vessel with 105° curvature.

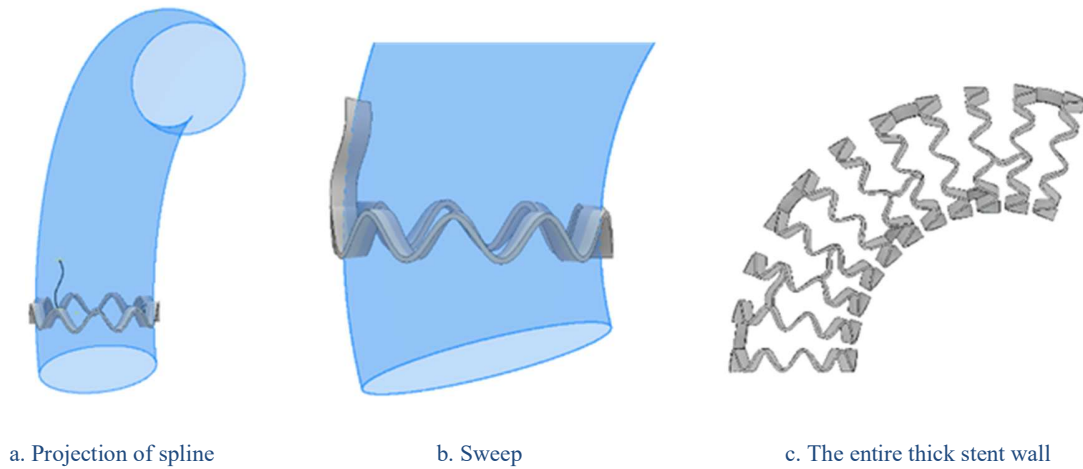


Figure 12 Generation of connectors

As the optimized stent geometry is obtained, a hollowed cube, whose thickness is equal to that of stent, is generated to intersect with the thick stent (figure 13. a.). This process yields an accurate stent geometry (Figure 13. b) which matches the stents shape in both curved vessels and vessels with bifurcation. Then, the flow domain can be obtained by subtracting the stent part from a curved cylinder model by this stent geometry (Figure 14.).

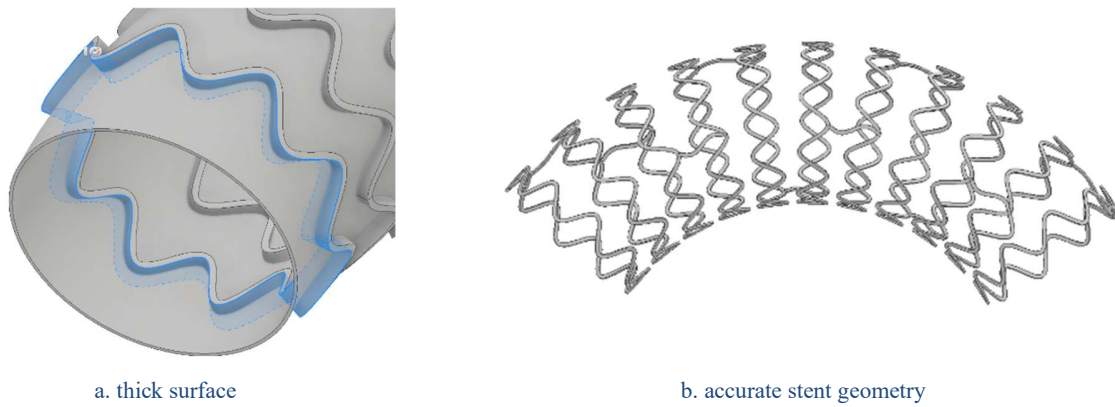


Figure 13 generation of stent ring

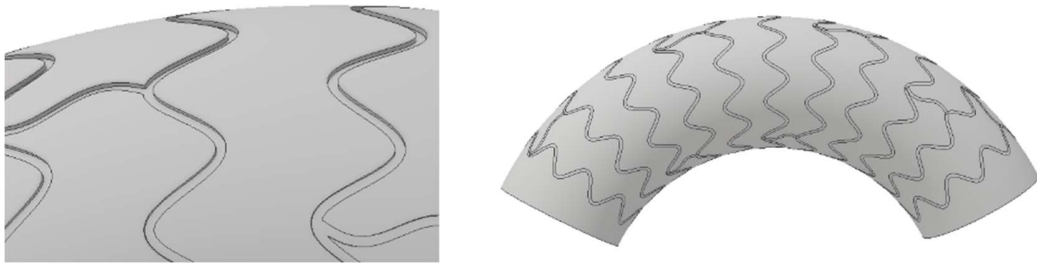


Figure 14 Substraction of stent

3.2 Computational Fluid Dynamics Analysis

Numerical simulations are performed using the commercially available Navier-Stokes solver ANSYS CFX (Canonsburg, PA). Blood is modelled using a laminar, Carreau-Yasuda non-Newtonian model [33]. The simulations are initially run as steady state, before being used as initiation for a transient solution to damp initial effects. The fourth cycle is used for the analysis of the simulation. Hemodynamic parameters such as the time averaged wall shear stress (TAWSS) and the velocity distributions are extracted from each of the simulations for comparison. Stent geometries are generated using AutoCAD Inventor (San Rafael, CA), which are then projected [32] onto the artery geometries using a Boolean approach to allow for the fluid volume to be meshed for all stented configurations.

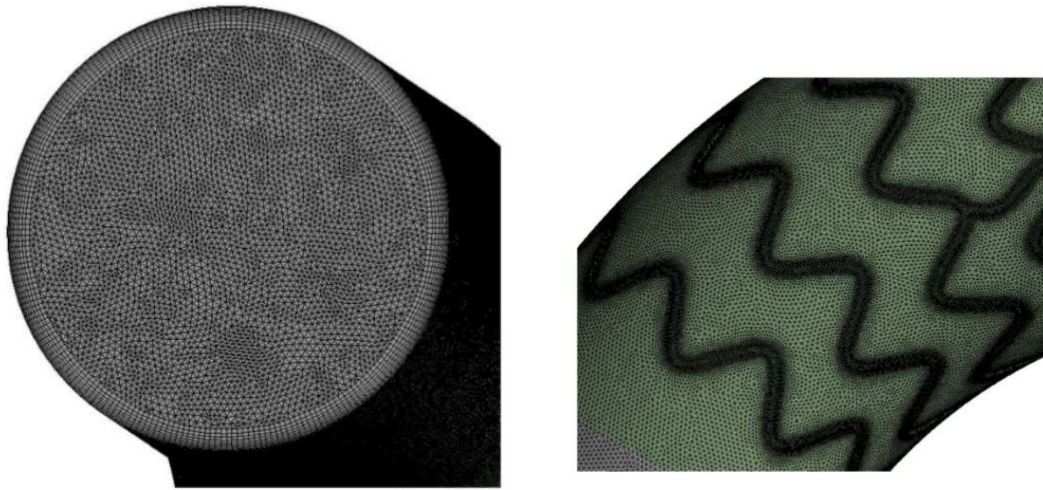


Figure 15 Face inflation (left) and edge size (right)

In ANSYS, geometry is divided into tiny mesh element for precise computation. In general, the size of element is set to be 0.05 mm. The software is set to capture curvature in geometries, which lead to a smoother mesh in the curved area. Thus, the value of the curvature captured is equal to the curvature of vessels. WSS is the focus point in this thesis, therefore, as shown in Figure 15, inflation function is applied to the surface of the blood flow domain to obtain more elements in this area. Besides, due to the existence of stent, the structure stent area is more complex, which needs finer elements to achieve valid result data. Figure 15. illustrates the result of Edge Sizing function applied to stent profile in flow domain. Thus, each geometry in this project has more than 6.5 million mesh elements and 17 million nodes to obtain an accurate result.

4. Results

Cross-sections located at the centre of curvature for the ideal cylinders and six locations for the ideal and patient-specific bifurcation models are chosen along the geometry to analyse and compare flow behaviour (Figure 16.). The velocity streamlines are plotted in all the chosen locations for each configuration along with TAWSS distributions. All the results are extracted at flow peak time (2.72 s)

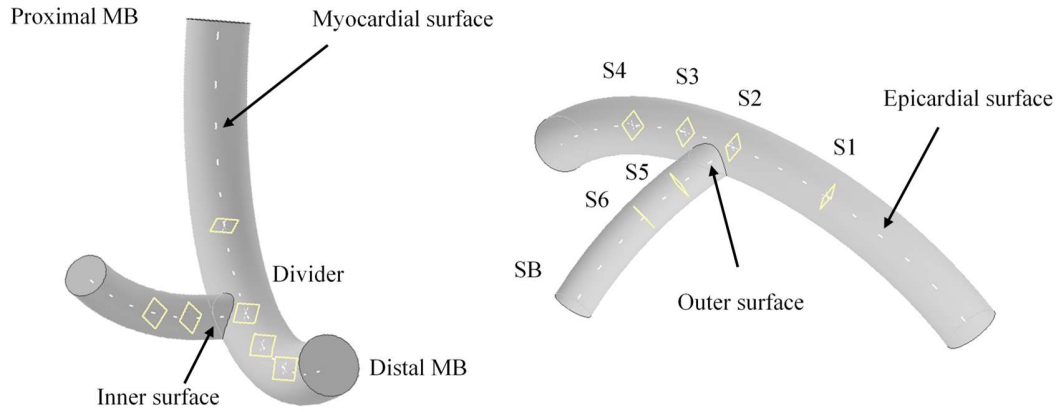


Figure 16 Cross-section planes defined in bifurcation models

4.1 Secondary flow

4.1.1 The influence of curvature on secondary flow

As patient-specific geometries have complex curvature condition, ideal cylinder and bifurcation angles are adopted to figure out the influence of curvature. The straight cylinder shows no secondary flow as expected, whereas the equivalent curved models show significant secondary flow vortices (Figure 18.) The flow in the cylindrical models, due to the changed vessel shape, moves from epicardial to the myocardial surface along the two sides of the vessel wall and returns inside the vessel. A pair of symmetric Dean vortices are formed on either side of the curvature normal (Figure 17). When the curvature is increased, the flow centre skews to the epicardial surface and the velocity profile turns to an apparent crescent shape (Figure 17).

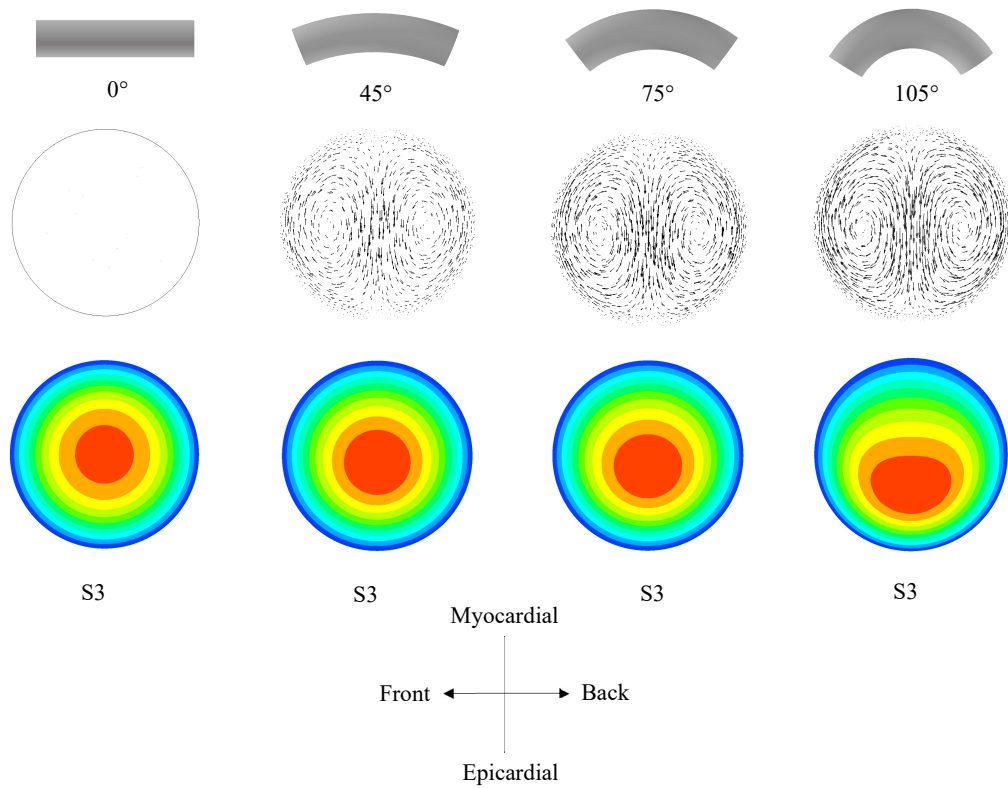


Figure 17 Dean-like flow in ideal cylinder models with different curvature

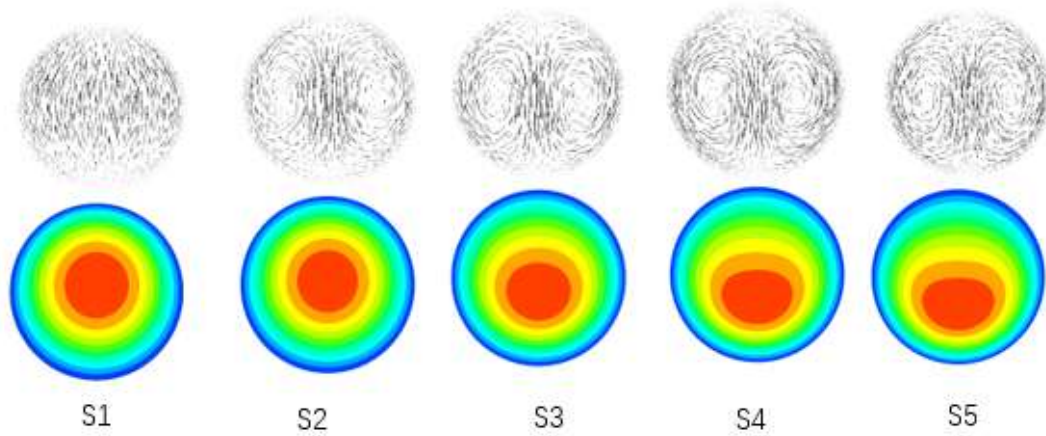


Figure 18 Dean-like flow in 5 cross-section planes of 105° ideal cylinder models

In the proximal main branch of the non-stented bifurcation models (Figure 19), Dean-like flow is observed with the velocity profile showing a similar characterization as that in ideal cylinder models (Figure 17.). A similar development of flow vortices is seen in the side branch, which is more pronounced in the patient-specific model with the vortices developing in an angular orientation before the divider i.e. in the proximal main branch (Figure 19.). After the flow splits due to the divider, flow separation and vortex formation takes place in addition to the secondary flow effects (Figure 20).

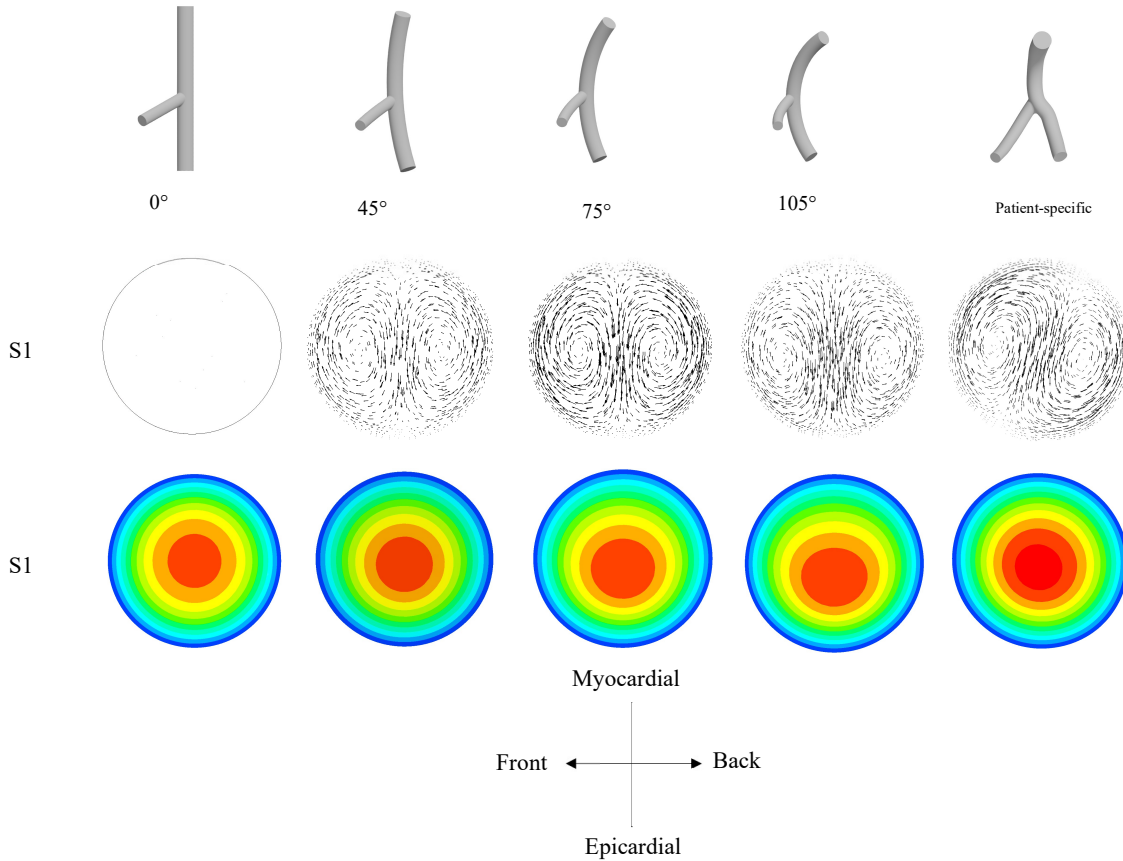


Figure 19 Dean-like flow in proximal MB (S1)

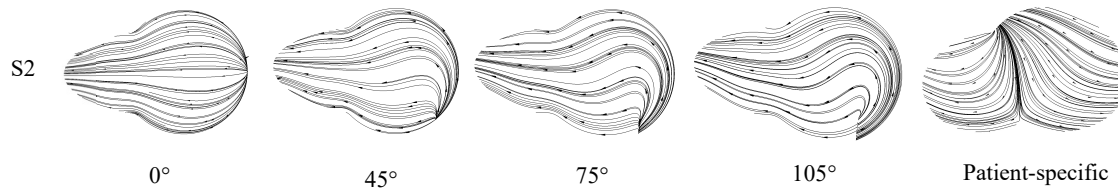


Figure 20 Dean-like flow in divider region (S2)

In Figures 21 and 22, fully developed Dean-like flows are shown to occur at several locations in the distal main branch and side branches of the bifurcation. In the first Dean-like flow (S3, S5), the flow moves from the inner to the outer surface and returns along the diameter. But the second Dean-like flow (S4, S6) shows an opposite orientation. In the ideal bifurcation model (non-curved), the pair of Dean-like flow vortices are symmetrical in the two daughter branches. In curved models, the vortices in daughter branches spin anticlockwise. The rotational amplitude of the first Dean-like flow (S3, S5) is relatively small, but the loss of symmetry is apparent. The vortex near the epicardial surface increases in size while the one near myocardial surface decreases, in both daughter branches. In the 105° curved model, the second Dean-like flow vortices (S4) in proximal MB are symmetrically present on the either side of the curvature normal in both daughter branches. Additionally, there is vortex dissipation in the side branches and secondary flow structures (Lyne-type and Wall-type) compared to the distal MB as shown in the cross-sectional flow structures at S5 and S6 as compared to S4.

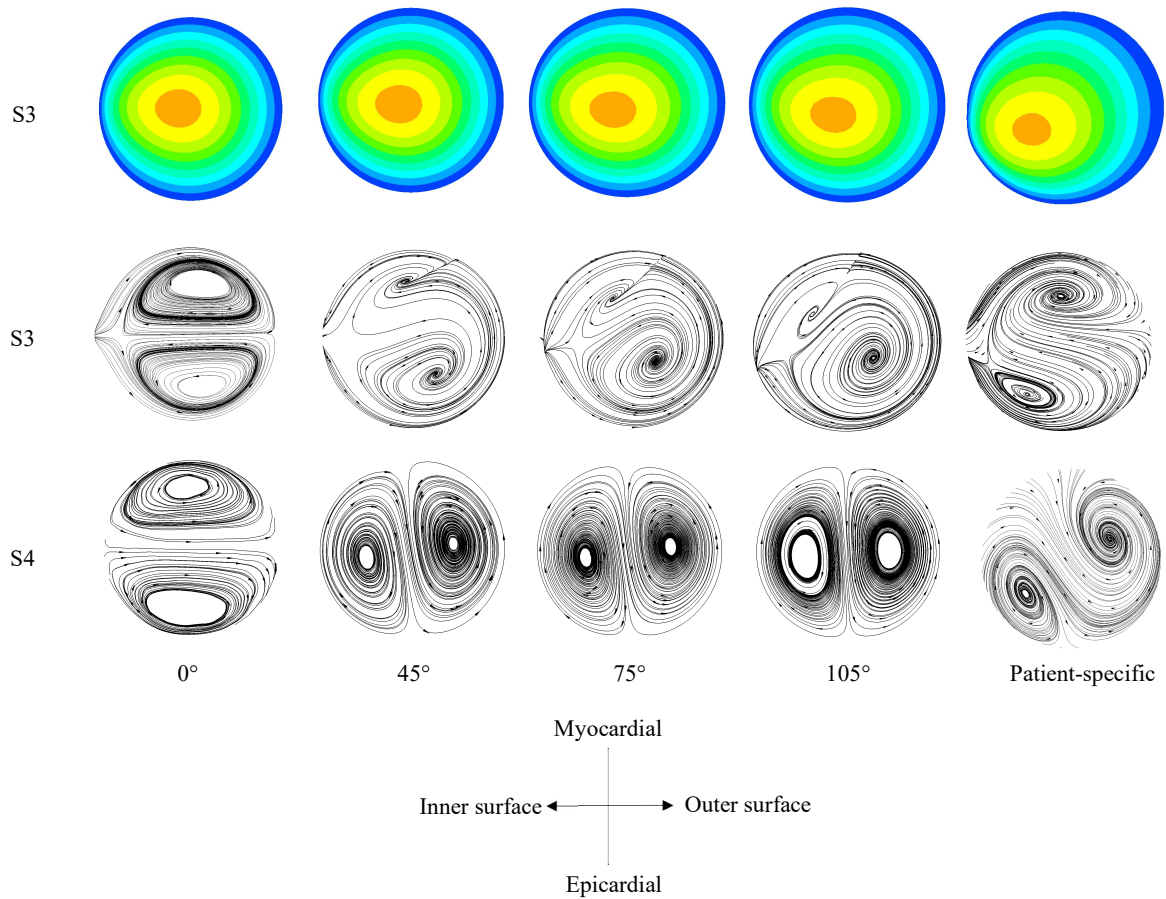


Figure 21 Velocity contour of S3 and Dean-like flow in distal MB(S3, S4) of non-stented bifurcations

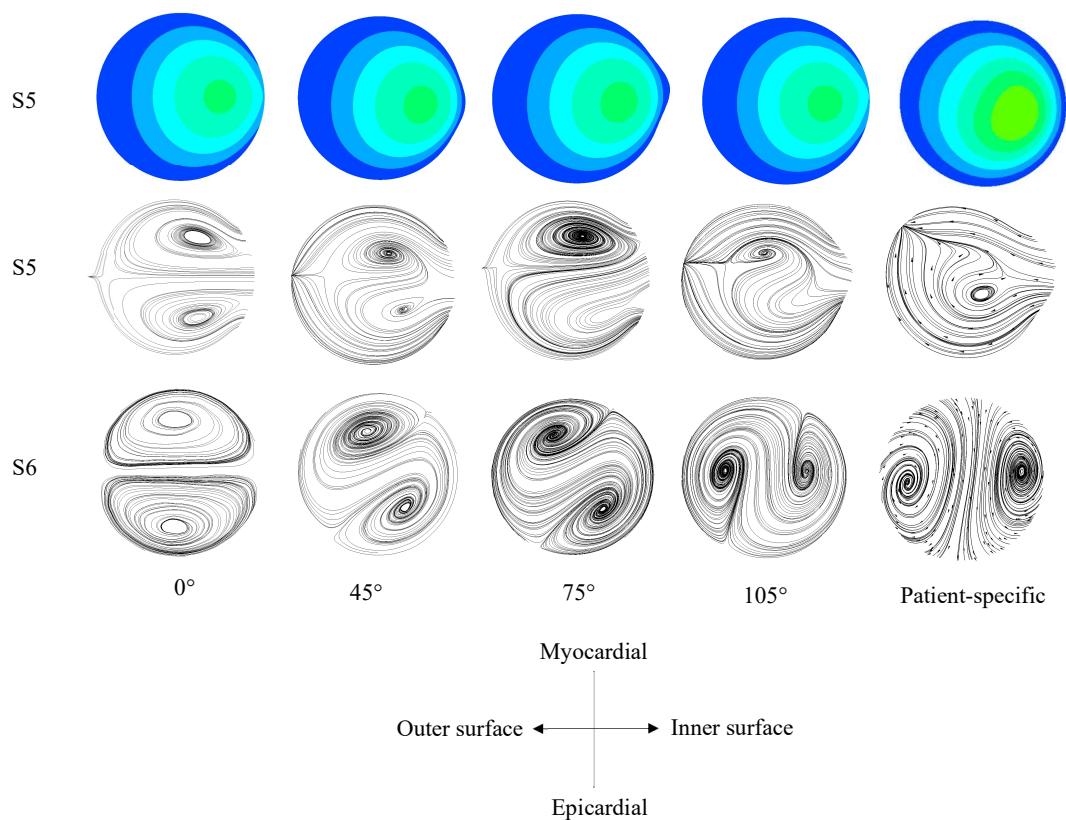


Figure 23 Velocity contour of S3 and Dean-like flow in SB (S5, S6) of ideal non-stented bifurcations with different curvature (0°, 45°, 75°, 105)° and 105° curved patient-specific model. The BA is fixed at 68°.

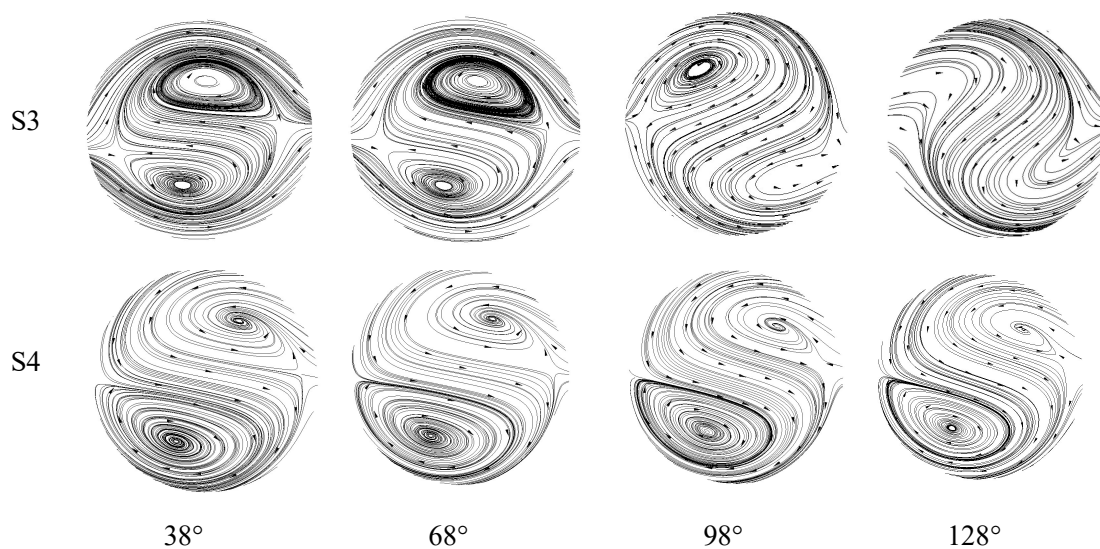


Figure 22 Dean-like flow in distal MB of 48° curved non-stented models with 38°, 68°, 98°, 128° BA

4.1.2 The influence of bifurcation angle on secondary flow

The figure 23. shows two Dean-like flows in S3 and S4 plane in 45° models with different BA. With the increase of BA, the first Dean-like flow becomes weak gradually, and in 128° BA models, the first Dean-like flow loses its typical shape with a large rotational amplitude. As talked before, the two Dean-like flow is generated by the bifurcation structure. The influence of bifurcation structure decreases with the BA increases. When BA becomes extremely large (128°), the Dean-like flow is significantly influenced by curvature, which results in the rotation and shape change. Conversely, the second Dean-like flow in S4, where the curvature already has visible influence, is not influenced by the variation of BA. The direction and shape have no apparent change.

4.1.3 The influence of stent on secondary flow

Stents in the MB were added to the previously simulated cylinder and bifurcations. Lyne type and Wall-type flow structures in the branches were seen in addition to the Dean type vortices (Figure 24.). The L-type and W-type vortices are formed due to dissipation of the Dean type vortices with the magnitude of curvature.

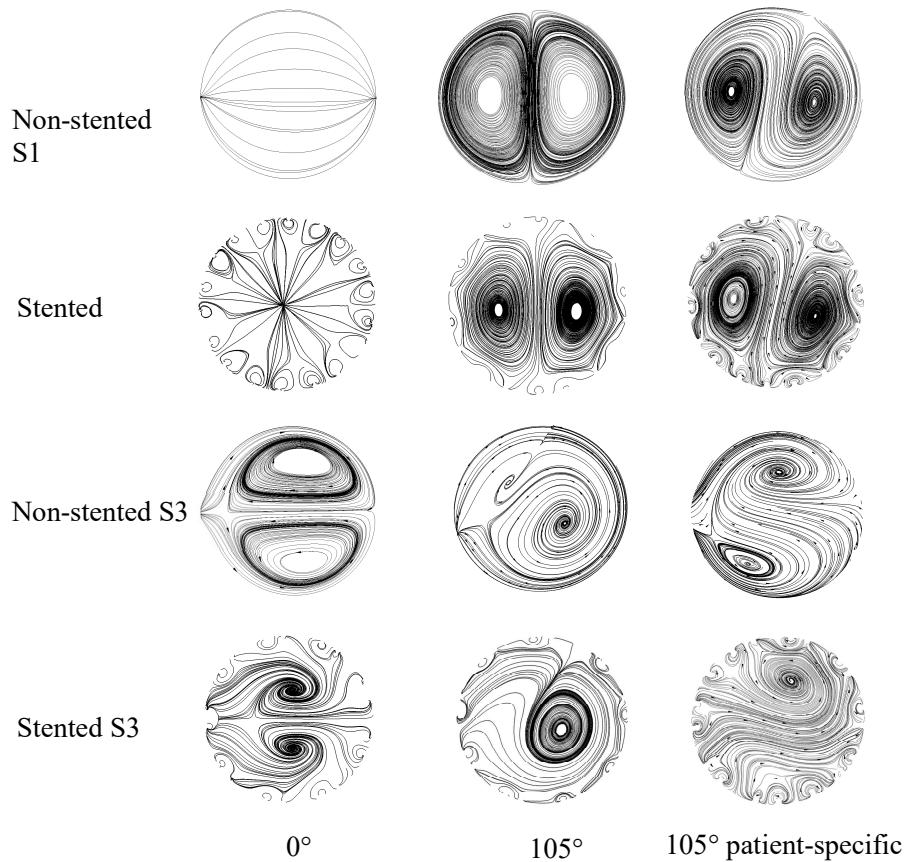


Figure 24 Comparision of non-stented and stented 105° curved models with 68° BA

4.2 WSS

4.2.1 The influence of curvature on WSS

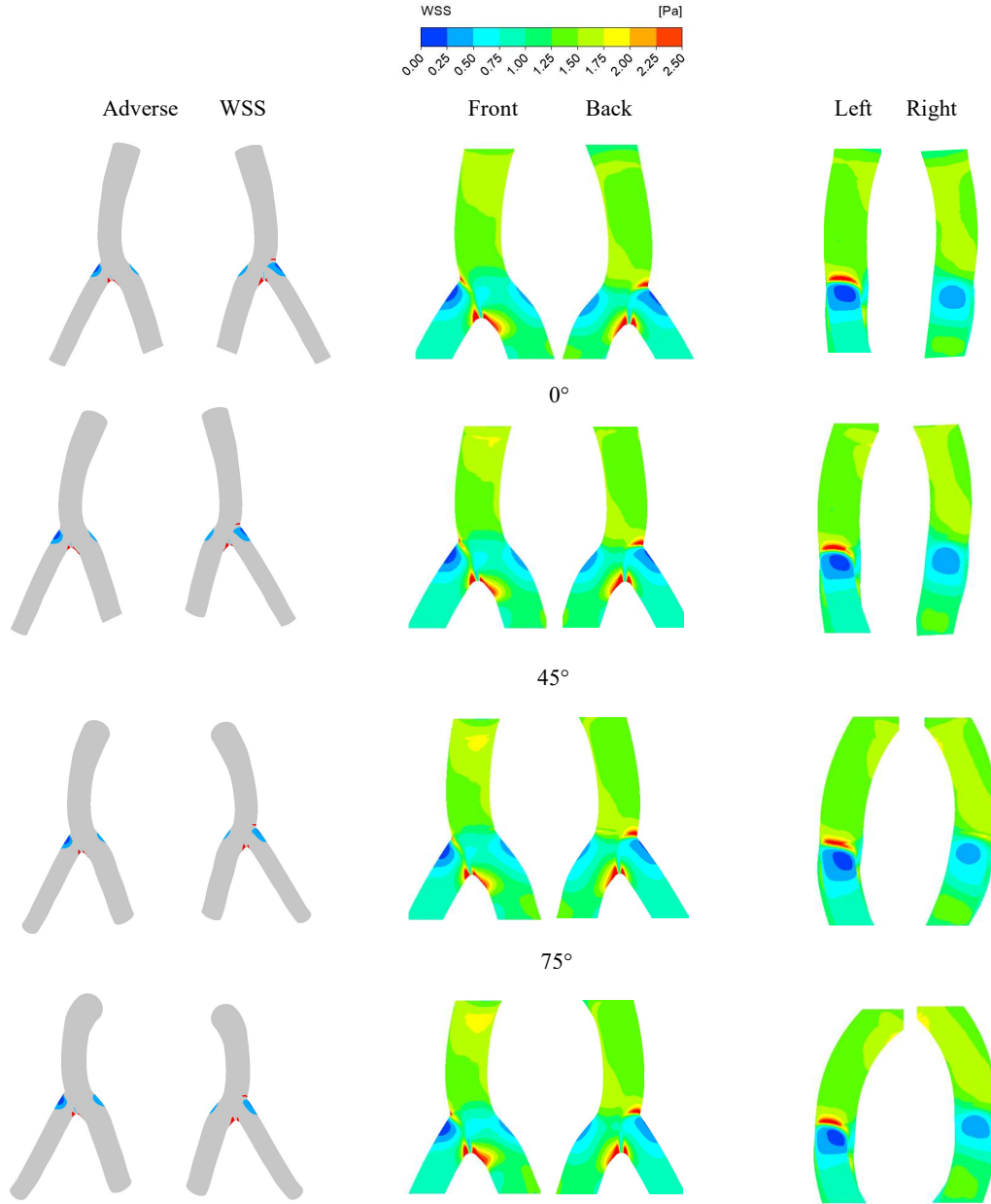


Figure 25 WSS distributions of 0°, 45°, 75°, 105° curved patient-specific bifurcation with fixed BA (68°) in front, back, left, right view and contours of adverse WSS

Figure 25. shows the WSS distributions when curvature changes with a fixed bifurcation angle (68°). The Low WSS region typically locates at outside surface of daughter branches (Figure 26. Left, right view), and high WSS locates at inner surface of daughter branches (Figure 26). A small region of high WSS locates at the outer side of proximal MB. The adverse WSS region shows a lower WSS in SB than that in MB. With

the increase of curvature, no apparent influence is found on high WSS area, however, the low WSS region tends to move to myocardial side (Figure 25 left, right view).



Figure 26 WSS distributions of 0° , 45° , 75° , 105° curved patient-specific bifurcation with fixed BA (68°) in bottom view

4.2.2 The influence of bifurcation angle on WSS

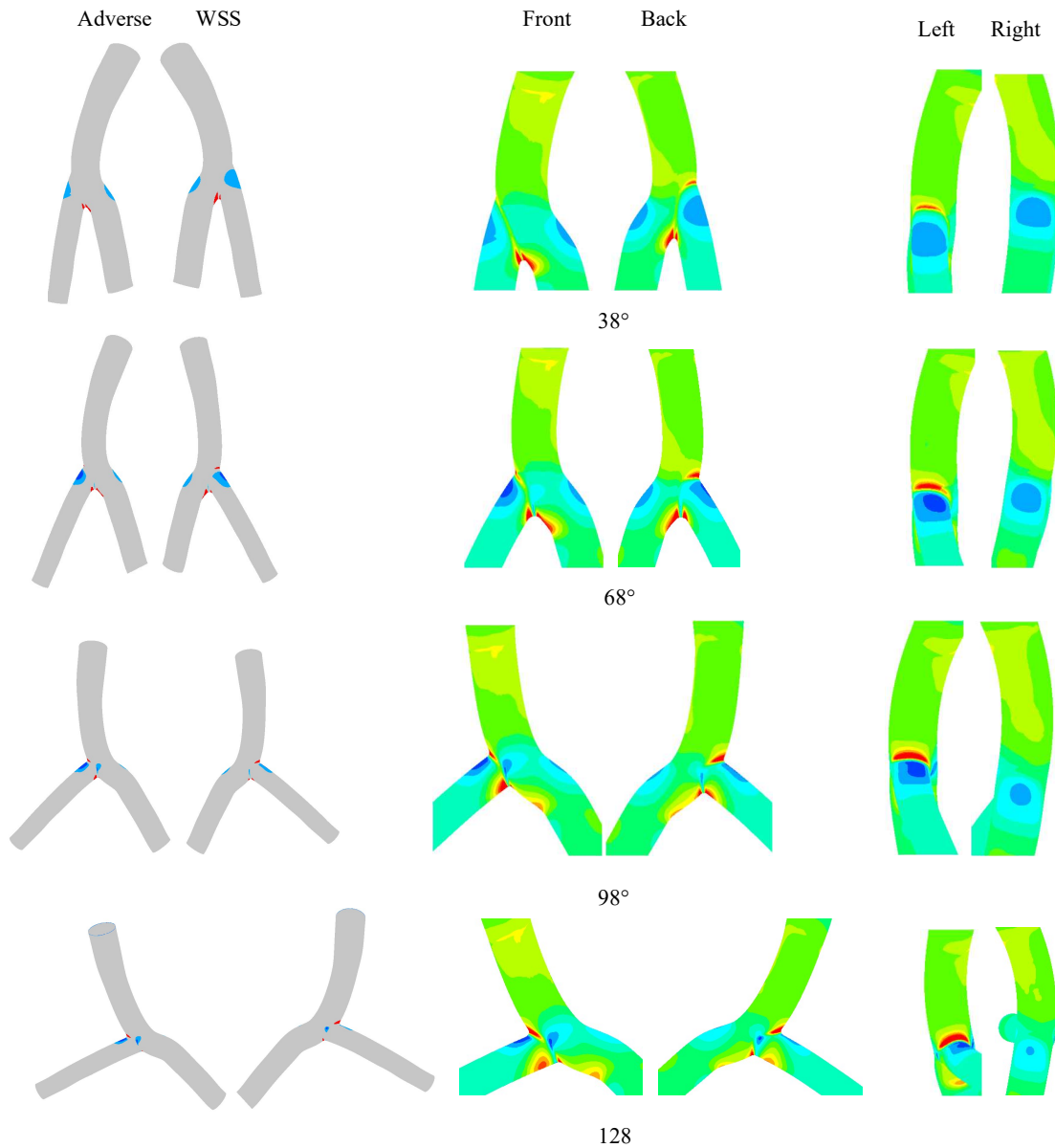


Figure 27 WSS distributions of 45° curved patient-specific bifurcation with 38° , 68° , 98° , 128° BA in front, back, left, right view and contours of adverse WSS

Figure 27. shows WSS distribution when bifurcation angle changes with a fixed curvature (45°). When bifurcation angle increases, the adverse WSS becomes lower but the low WSS area increases on the outside surface in daughter branches (Figure 27 left, right view). Large high WSS area can be found in 45° and 75° BA models (Figure 28). Conversely, in 128° bifurcation angles, it can be discovered that the adverse high WSS area in SB disappears, and only small region exists in distal MB.

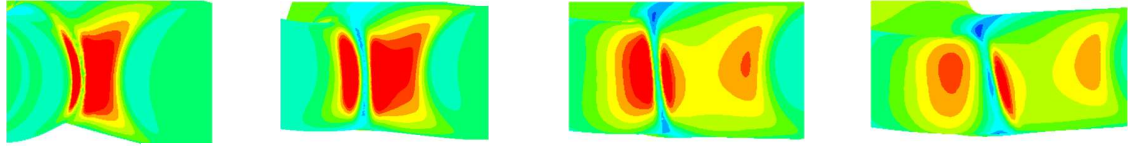


Figure 28 WSS distributions of 45° curved patient-specific bifurcation with 38° , 68° , 98° , 128° BA in bottom view

4.2.3 The influence of stent on WSS

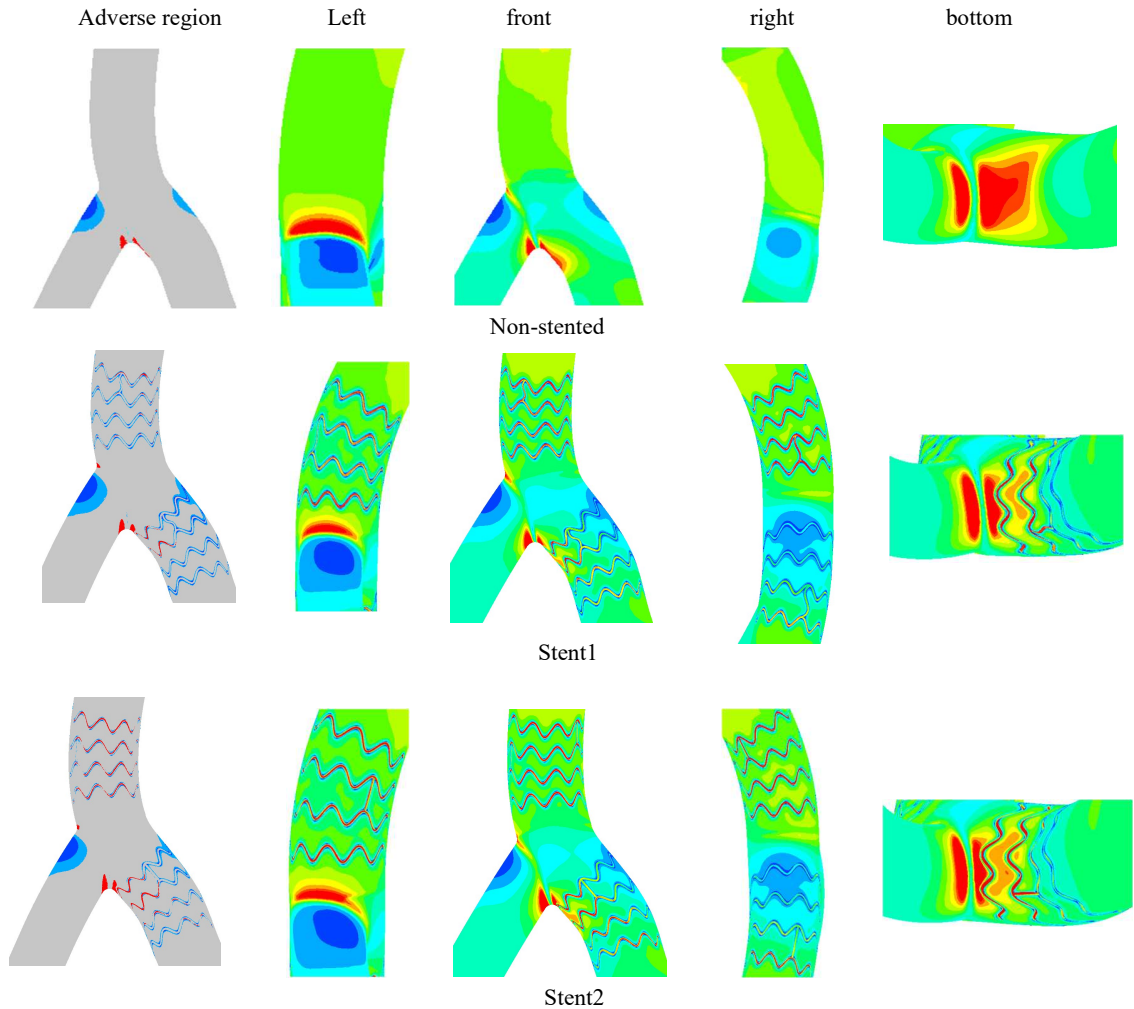


Figure 29 WSS distributions of 45° curved patient-specific bifurcation with 38° , 68° , 98° , 128° BA in front, left, right, bottom view and contours of adverse WSS

When vessels are stented, additional low WSS happens around the stents and high WSS exists in the stented area (Figure 29.). The area covered by stents has a lower WSS distribution. The typical low WSS region on the outer surface of distal MB near divider extends to the stented area. However, the stents only influence local region, and WSS distribution in non-stented region keeps the same (figure 29 left view). When comparing two types of stents, larger low WSS area exists in the models with stent 1. However, there is more high WSS area in stented area in models with stent 2.

The clustered column charts below quantitatively compares the percentage area of adverse low (<0.5 Pa) and high WSS (>2.5 Pa) for all models based on the flow peak time (2.72s) to figure out the comprehensive influence of each parameter. Compared with curvature, the bifurcation angle has more significant influence on low WSS area. As shown in these charts, the increased bifurcation lowers down the percentage low WSS area level for models with all curvature. It can be discovered that, the percentage high area is slightly larger in 68° and 98° BA models. The influence of curvature is not clearly when comparing the percentage area, thus, curvature may have limited influence on adverse WSS region size.

It is apparent that the exist of stents brings significant impact on adverse WSS region. Both low and high WSS increase when the model is stented. The low WSS around the stents and high WSS in the area covered by stent body directly raise the adverse WSS percentage area. The stent 1 which has a rectangle cross-section arouses more low WSS, compared with stent 2 which has a circular cross-section. Conversely, thicker stent 2 results in more high WSS in stented area.

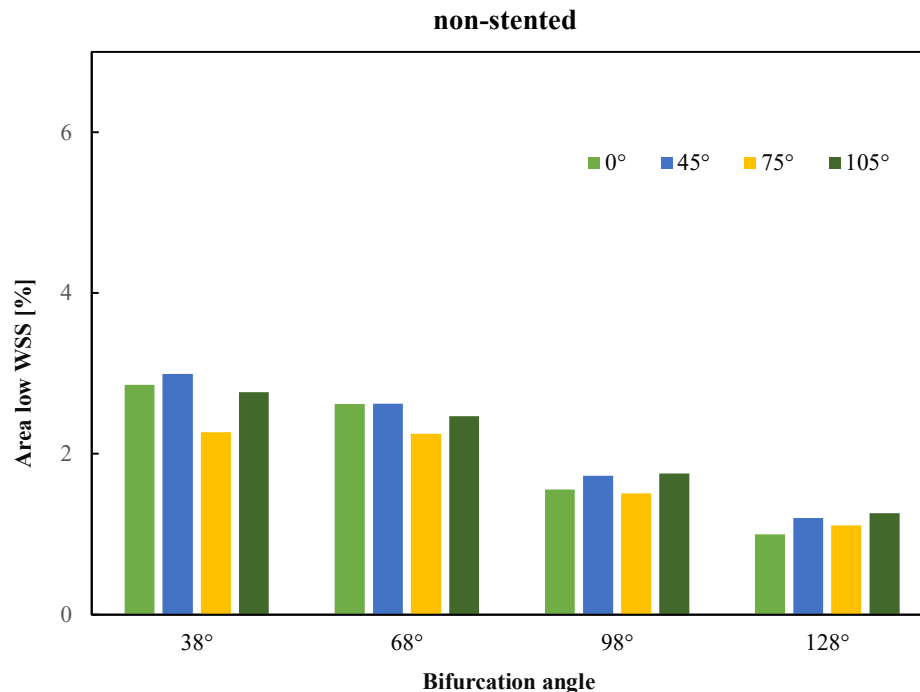


Figure 30 Percentage of low WSS area of non-stented patient-specific bifurcations

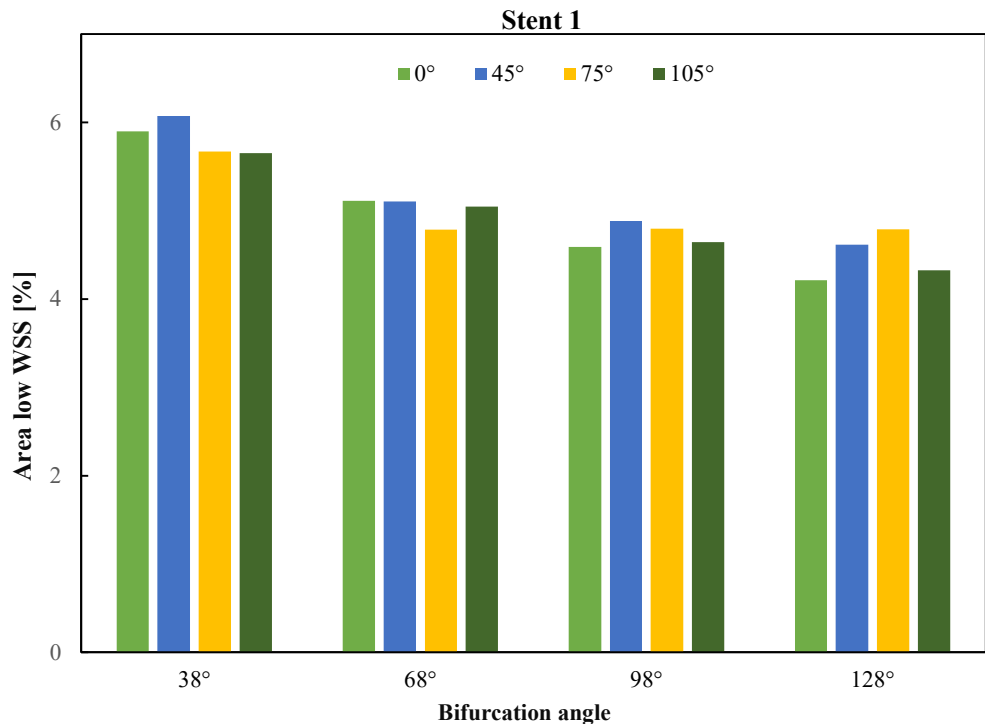


Figure 31 Percentage of low WSS area of patient-specific bifurcations with stent 1

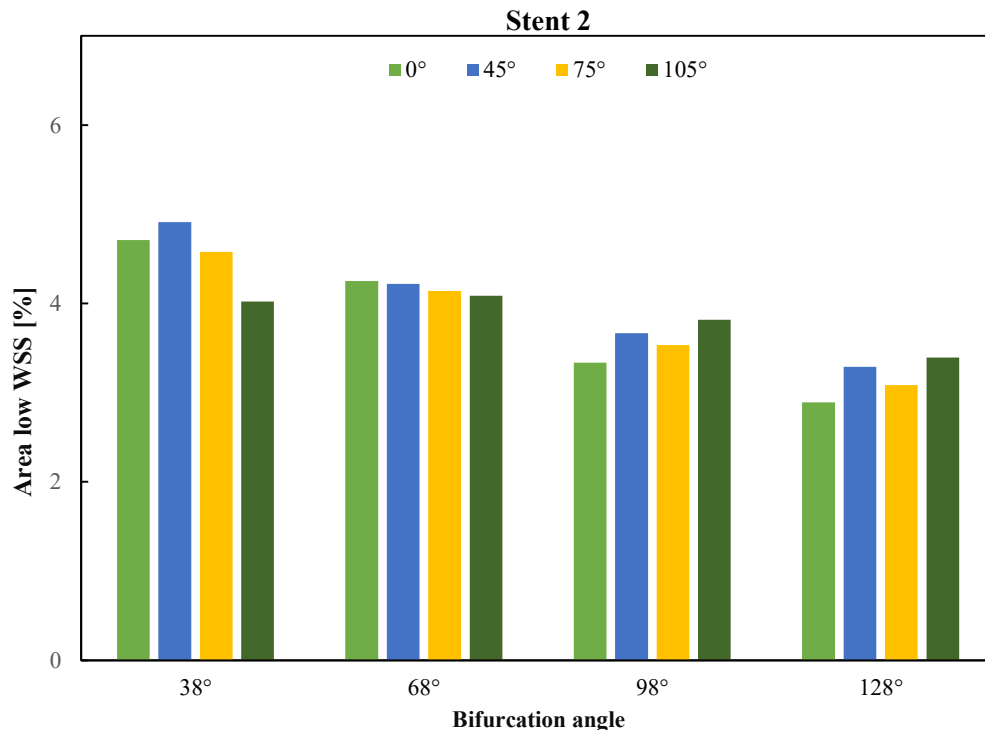


Figure 32 Percentage of low WSS area of patient-specific bifurcations with stent 2

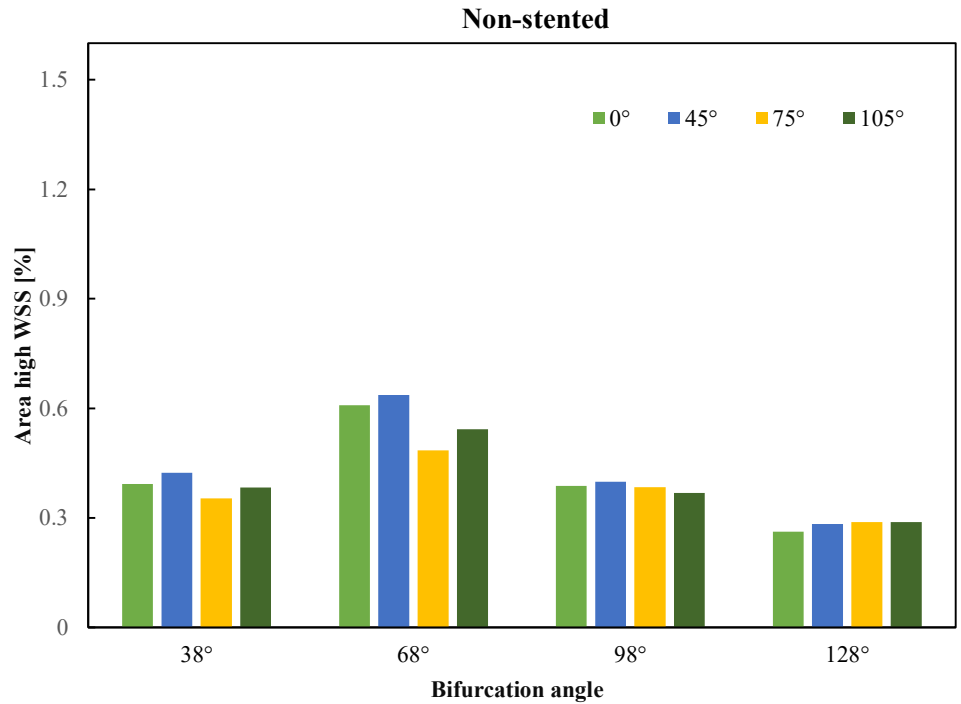


Figure 34 Percentage of high WSS area of non-stented patient-specific bifurcations

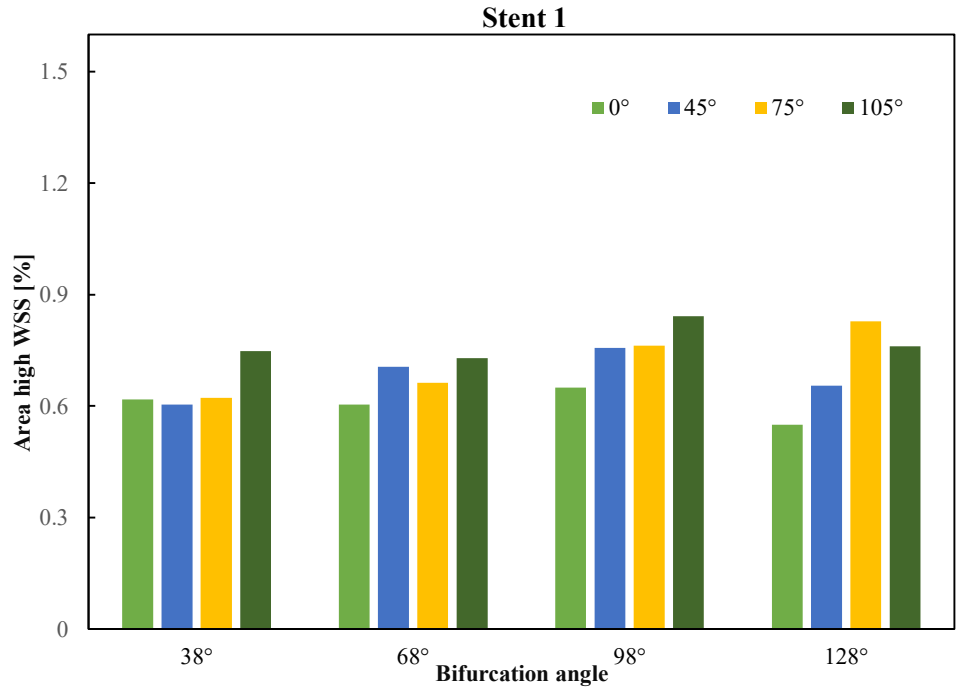


Figure 33 Percentage of high WSS area of patient-specific bifurcations with stent 1

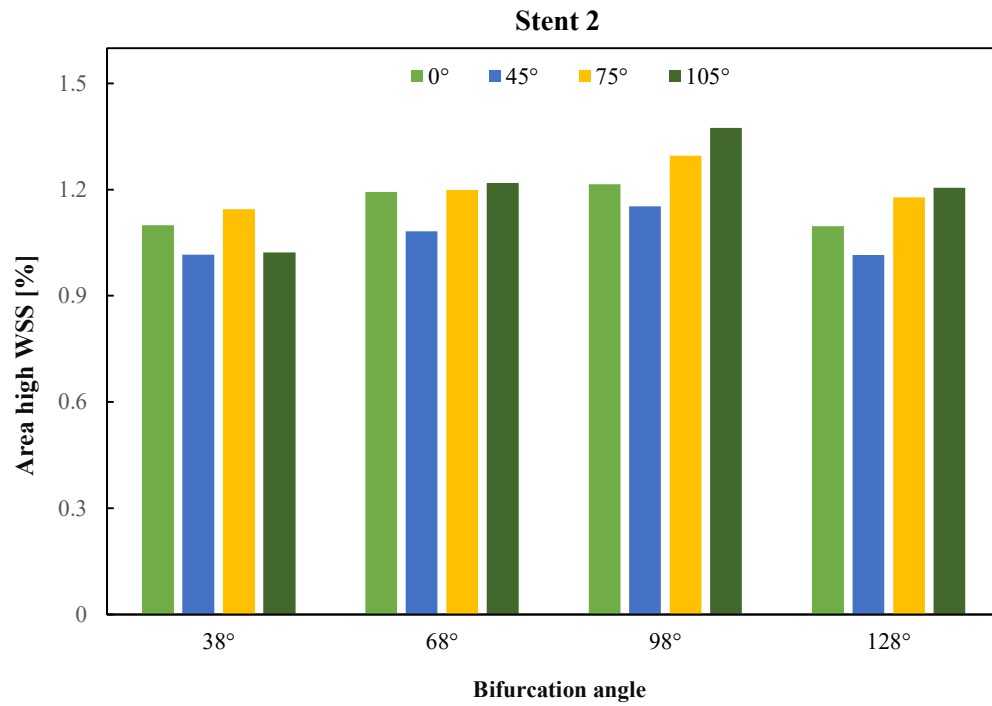


Figure 35 Percentage of high WSS area of patient-specific bifurcations with stent 2

4.3 TAWSS

4.3.1 The influence of curvature on TAWSS

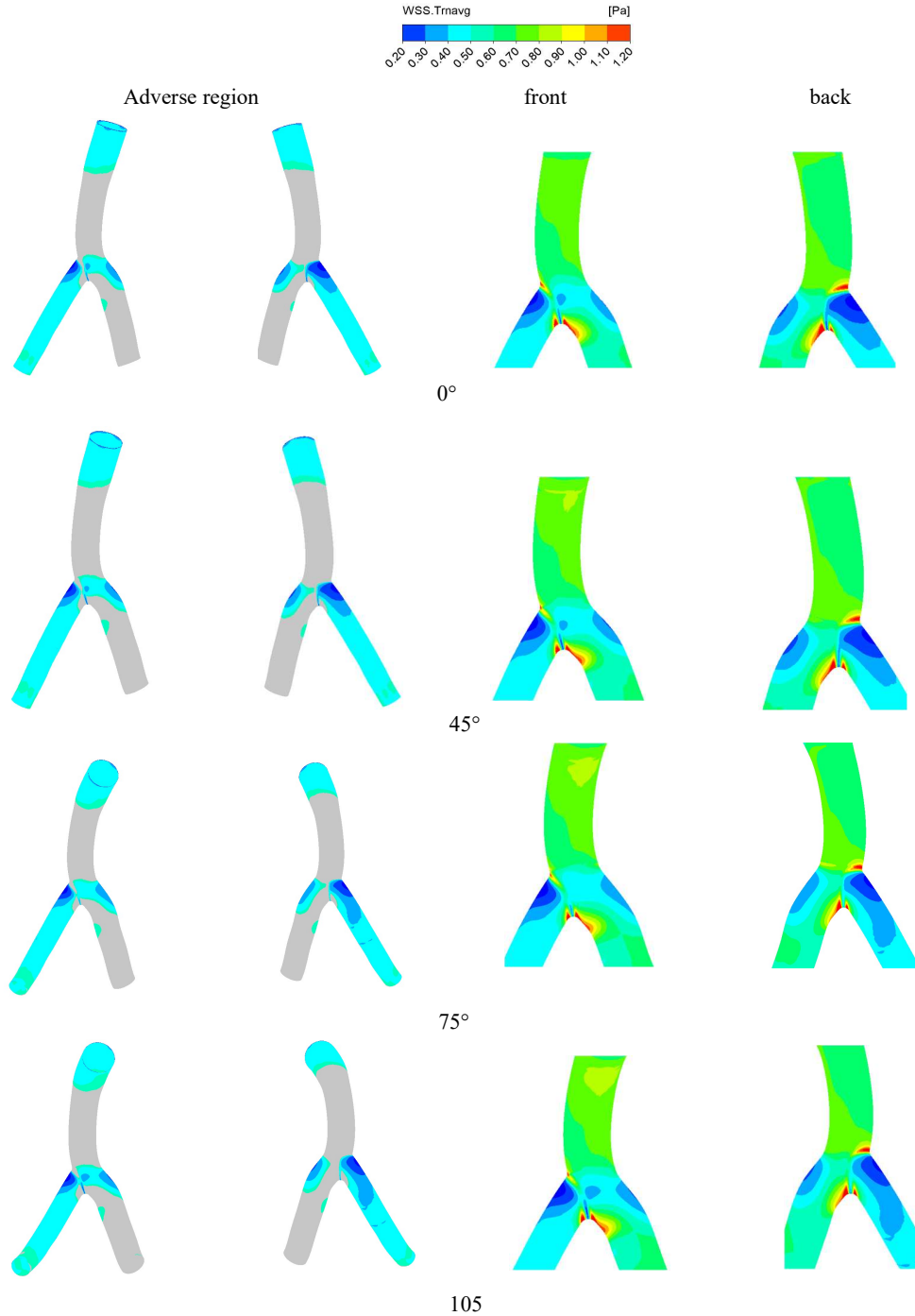


Figure 36 TAWSS distributions of 0°, 45°, 75°, 105° curved patient-specific bifurcation with fixed BA (68°) in front, back view and contours of adverse WSS

The figure 36 shows the low TAWSS distribution when curvature changes with a fixed BA (68°). The inherent curvature and bifurcation structure in patient-specific bifurcations means that secondary flow vortices form in daughter branches and influenced by curvature thereby predisposing the site to adversely low TAWSS and hence plaque deposition. The first Dean-like flows (S3, S5) generated by bifurcation structure directly affects TWSS distribution at outer surface of daughter branches where apparent low TAWSS locates. According to streamline plot of S2 (Figure 20.), since the flow division in the bifurcation divider area, low TAWSS happens in both myocardial and epicardial surface, and the low TAWSS region covers the whole SB due to less flow entering. The influence of curvature is apparent that the low TAWSS region moves from epicardial surface to myocardial surface in divider region where streamline is also influenced by curvature, and in large curvature model (105°), no low TAWSS is discovered in epicardial surface. With the increase of curvature, the symmetry loss and rotation of the first Dean-like flow (S3) leads that low TAWSS region in SB on the outer surface extends to epicardial surface. The second Dean-like flow (S4) in distal MB which has an opposite flow direction from the first one (S3) consequently result a low TAWSS on the inner surface downstream the distal MB.

4.3.2 The influence of bifurcation angle on TAWSS

The figure 37. shows the low TAWSS distribution when BA changes with a fixed curvature (65°). It is apparent that the low TAWSS area on outer surface decreases with the increasing BA, especially in distal MB. With the increase of BA, the first Dean-like flow gradually becomes weak (Figure 23. S3), which means the influence of bifurcation structure decreases. As seen in the figure 38, low TAWSS region appears and grows with the increase of BA at the corner of two side branches. No apparent influence is found on the low TAWSS region on the inner surface in distal MB due to less change of the second Dean-like flow (Figure 23. S4).

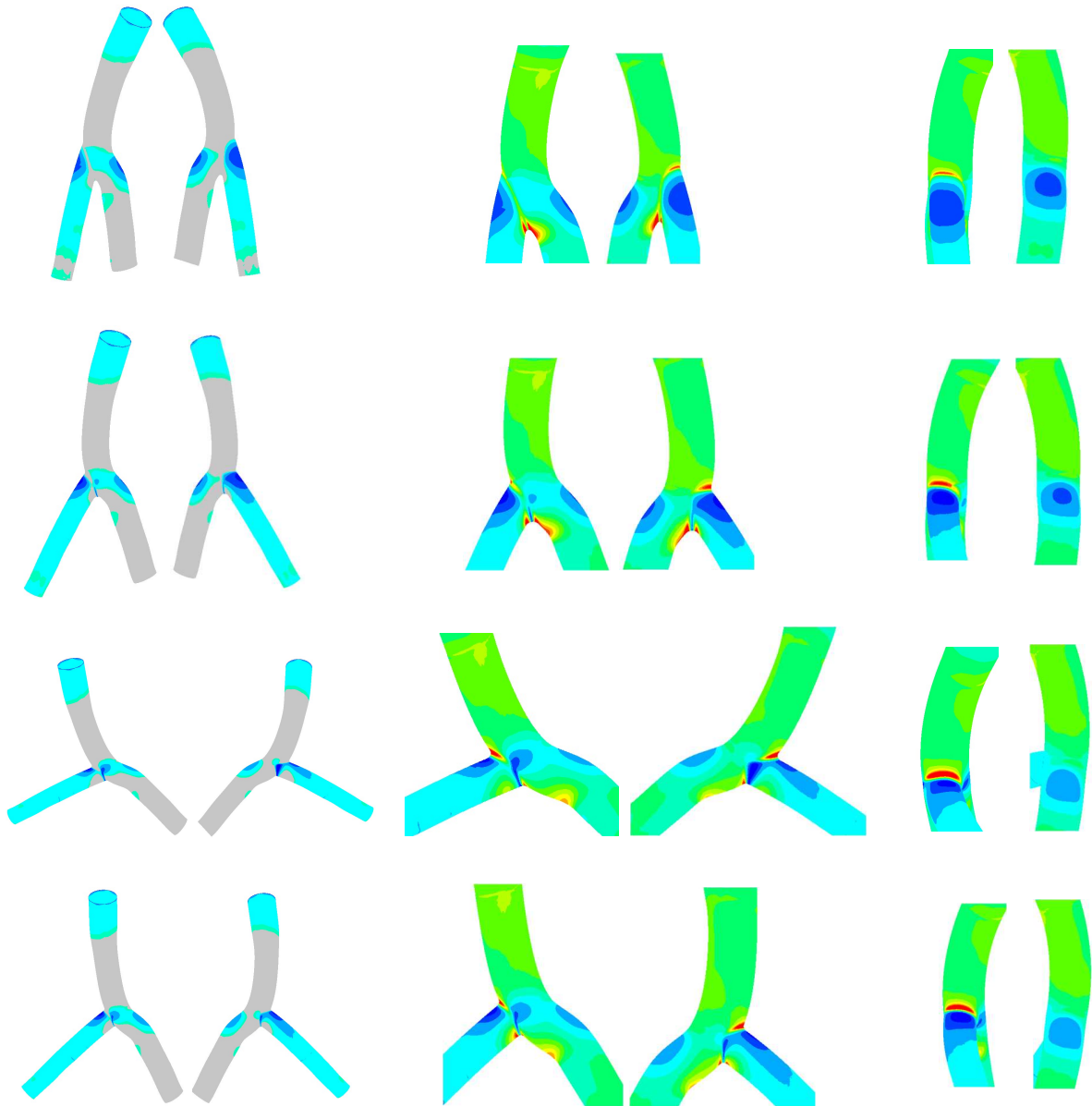


Figure 37 TAWSS distributions of 45° curved patient-specific bifurcation with 38°, 68°, 98°, 128° BA in front, back, left, right view and contours of adverse WSS

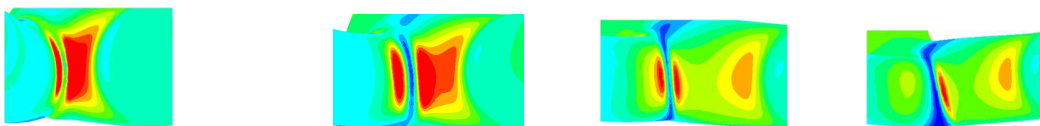


Figure 38 TAWSS distributions of 45° curved patient-specific bifurcation with 38°, 68°, 98°, 128° BA in bottom view

4.3.3 The influence of stents on TAWSS

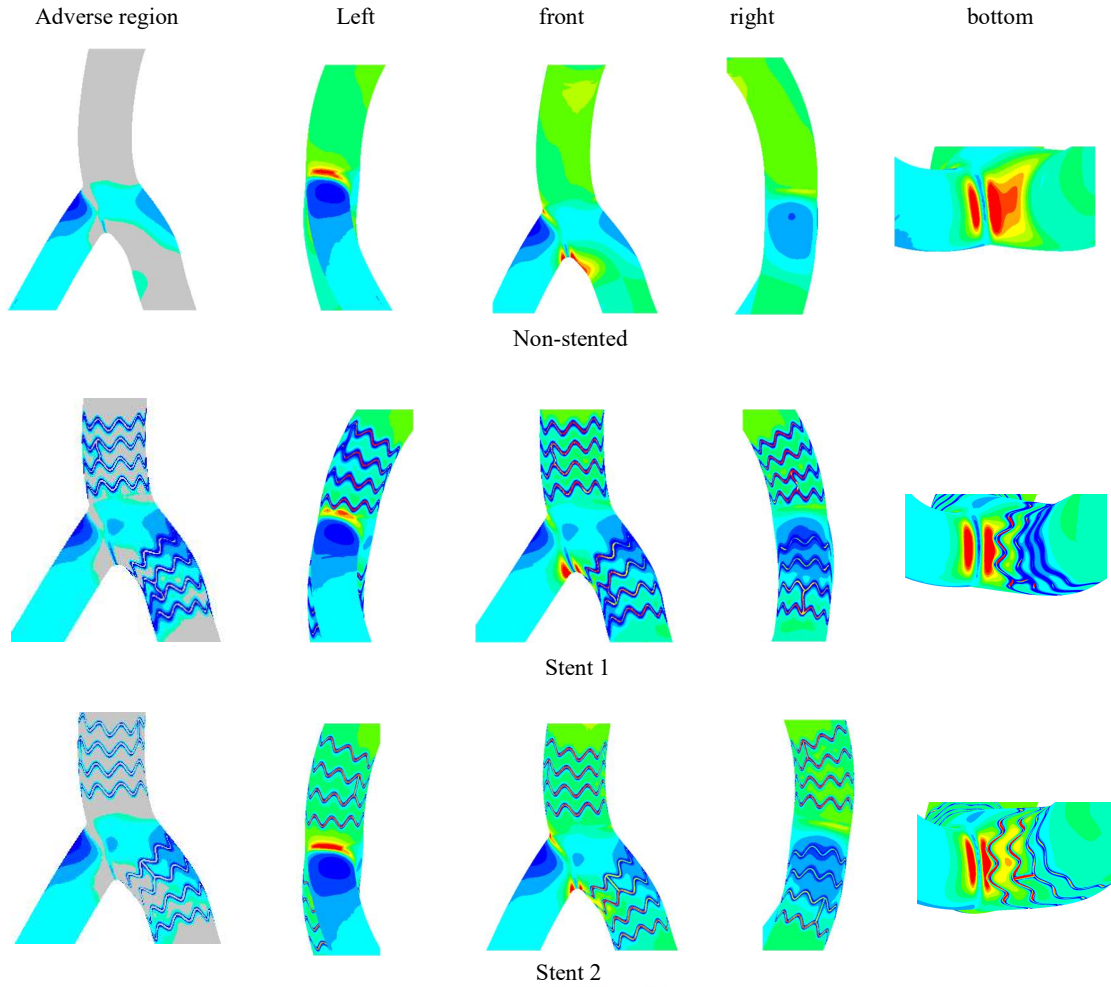


Figure 39 TAWSS distributions of 45° curved patient-specific bifurcation with 38°, 68°, 98°, 128° BA in front, left, right, bottom view and contours of adverse WSS

The small-scale secondary flow around the stents body (Figure 24.) arouse adverse TAWSS region (Figure 39.) around the stent. As seen in Figure 24, the small secondary flow influences Dean-like flow profile (S3), thus, the low TAWSS on the outer surface extends to the stented region. The stent 1 (rectangle) results in larger low TAWSS around the stent body.

According to the clustered column charts below, the low TAWSS aroused by stents directly increase the percentage low TAWSS area. The circular cross-section (stent 2) results in less TAWSS region than the rectangle one (stent 1). Narrow BA (38°) leads to the least adverse TAWSS area. However, the percentage low TAWSS area raises and is highest in 68° BA, and then, decrease with the increasing BA. The influence of curvature is still unclear based in the percentage area data, but 45° curvature leads to larger percentage low TAWSS area in stented models.

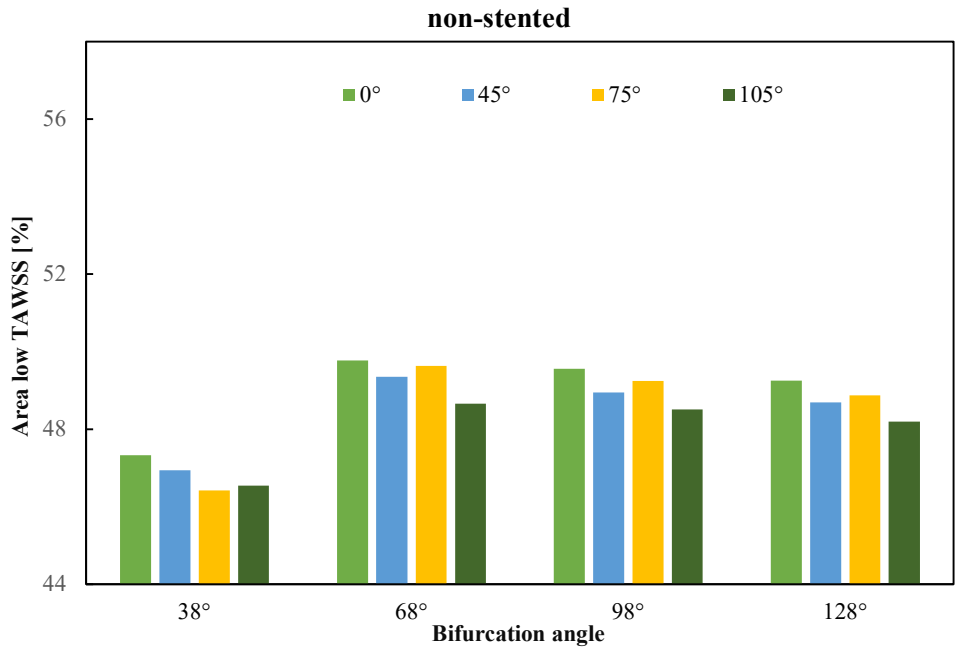


Figure 40 Percentage of low TAWSS area of non-stented patient-specific bifurcations

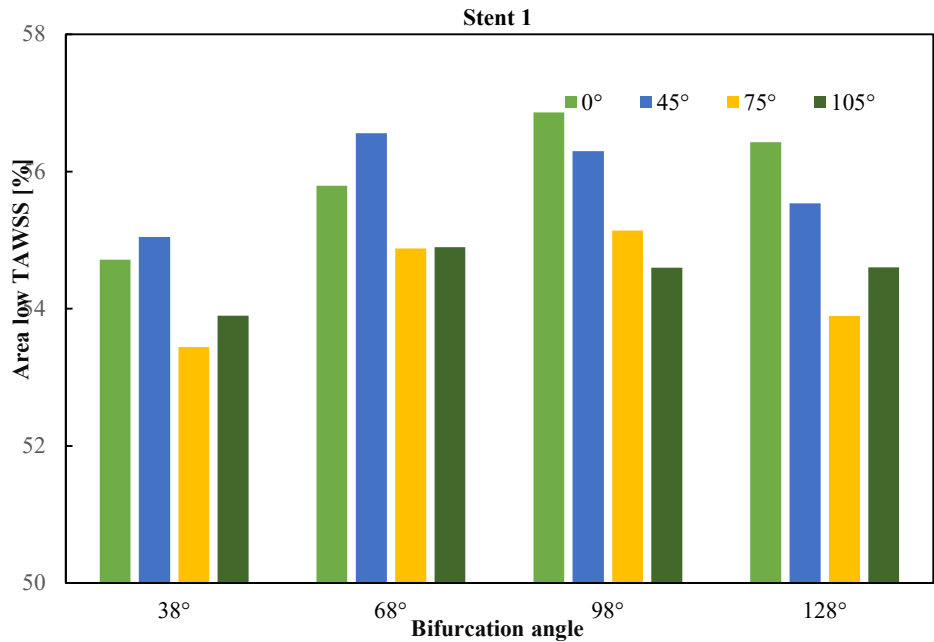


Figure 41 Percentage of low TAWSS area of patient-specific bifurcations with stent 1

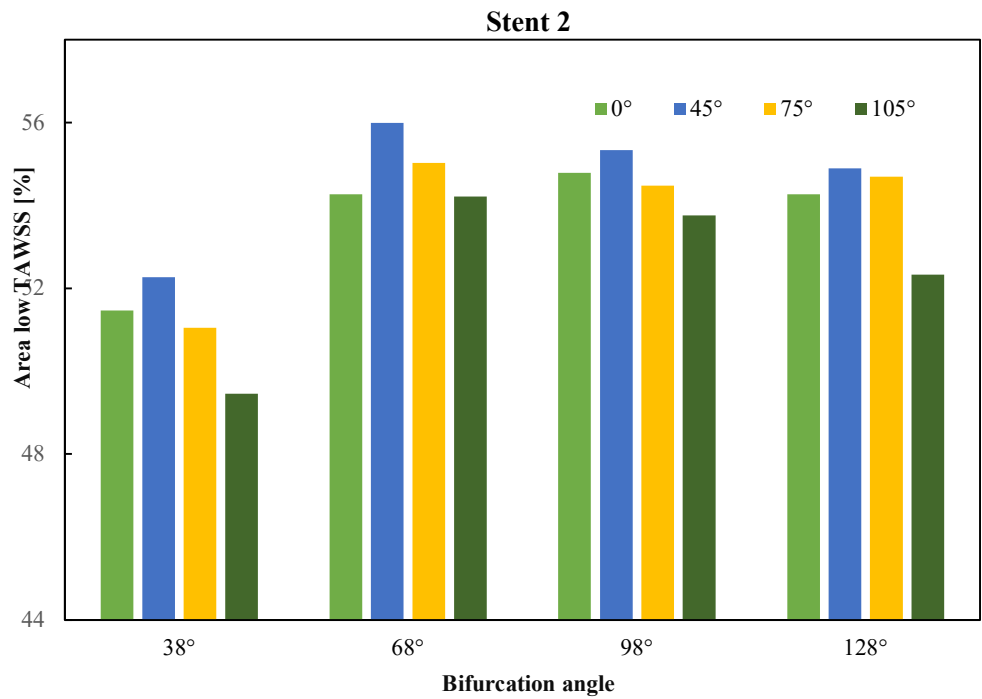


Figure 42 Percentage of low TAWSS area of patient-specific bifurcations with stent2

5. Discussion

An understanding of the effect of curvature, bifurcation and stenting on coronary arteries is essential in understanding coronary haemodynamics. Curvature is known to be the primary factor in secondary flow development [21, 25]. Our simulations involving both idealised and patient-specific bifurcation configurations show significant influence of curvature in generating Dean-like flow in the proximal MB and a pair of Dean vortices in each daughter branch (SB) for a range of curvatures investigated. Flow in the unstented proximal MB is mainly influenced by curvature and can be considered as being equivalent to a cylinder as it shows similar secondary flow structures as well as TAWSS distribution. The identified vortex skewing and loss of symmetry in bifurcations agrees with previous findings in addition to the secondary flow structures in the SB involving L-type and W-type vortex structures as seen by Bulusu and Plesniak [13]. The flow vortices in each case of curved arteries tend to skew to the epicardial surface of the curvature, and Dean-like flow tends towards becoming more asymmetric, which result the skewing of low TAWSS distribution on outer surface near divider (Figure 37). The vortex near epicardial surface tends to dominate the secondary flow field. With the increase of curvature, the influence of curvature on the Dean-like flow generated by bifurcation structure will increase, which has been already proved by a previous study [24]. Furthermore, the increased curvature will gradually control the Dean-like flow with the increase of distance from divider in the distal MB. Although the influence of curvature is significant according to the S3 velocity contour (Figure 21 S3.), the bifurcation structure determines the typical velocity distribution in daughter branches near the divider and the influence of bifurcation is also more apparent than other parameters on percentage low TAWSS area. Following on from Weydahl et al. [34], high shear rates occur on the inner surface while low shear rate on the outer surface leading to high and low TAWSS regions, respectively. The low TAWSS regions promote atherosclerotic plaque deposition. With the increase of bifurcation angle, the influence of bifurcation structure decreases resulting less adverse TAWSS region on outer surface near divider.

The influence of stents is significant on Dean-like flow in ideal cylinder and proximal MB in bifurcations. Additionally, in distal MB, the presence of stents changes the Dean-like flow structures. Following from [13], there is a significant flow breakdown and sub-structures of the flow such as L-type and W-type vortices are formed. These are in addition to the eddies formed around the stent struts as shown in Figure 24. for the cross-section S3. These flow structures warrant future work on the flow development downstream of stents. The significant effect of placing stents in the bifurcation is the development of a low TAWSS region making it predisposed to atherosclerotic plaque deposition and thus may present an important clinical insight.

In this project, the vessel geometry is rigid and no atherosclerotic plaque is considered in vessels. Besides, the blood flow is pulsatile, but this project only focus on the peak flow time point (2.72s). The future work

can focus on results at different time points during the cardiac cycle to achieve a more realistic understanding.

6. Conclusion

The effect of curvature and bifurcations on the development of secondary flows in different bifurcation configurations are investigated with and without stents. Ideal cylindrical, ideal bifurcating and patient-specific bifurcating vessels are simulated using computational fluid dynamics (CFD). The results demonstrated the significant effect of curvature on secondary flow vortices and thus TAWSS in these regions. The results showed that bifurcation structure and presence of vessel curvature generates Dean-like flow in all configurations; leading to the development of two pairs of Dean vortices in each of the daughter branches in the case of bifurcating vessels, and additional flow structures in the region around stents, that affect the Dean vortex pairs. The presence of stents has a significant effect on the developed flow fields in all models. Dean's vortices generated due to the vessel geometry are an important fluid dynamic effect that need to be considered in the context of coronary artery disease with a direct relevance for the understanding of atherosclerotic plaque development. This project significantly improves the understanding of the flow fields in complex coronary bifurcation geometries which has not been studied to this extent before. Novel findings regarding the impact of stents in such complex geometries has also been shown for the first time. Together, this contributes to greater knowledge on haemodynamics in coronaries and may help to understand atherosclerosis development in future.

References

- [1] G. A. Fishbein, M. C. Fishbein, and L. M. Buja, "Chapter 7 - Myocardial Ischemia and Its Complications," in *Cardiovascular Pathology (Fourth Edition)*, L. M. Buja and J. Butany, Eds. San Diego: Academic Press, 2016, pp. 239-270.
- [2] D. E. Newby and K. A. A. Fox, "Chapter 8 - Stable Ischemic Heart Disease/Chronic Stable Angina," in *Cardiovascular Therapeutics: A Companion to Braunwald's Heart Disease (Fourth Edition)*, E. M. Antman and M. S. Sabatine, Eds. Philadelphia: W.B. Saunders, 2013, pp. 131-152.
- [3] D. S. Krantz and N. R. Lundgren, "8.08 - Cardiovascular Disorders," in *Comprehensive Clinical Psychology*, A. S. Bellack and M. Hersen, Eds. Oxford: Pergamon, 1998, pp. 189-216.
- [4] B.-H. Toh, T. Kyaw, P. Tipping, and A. Bobik, "Chapter 71 - Atherosclerosis," in *The Autoimmune Diseases (Fifth Edition)*, N. R. Rose and I. R. Mackay, Eds. Boston: Academic Press, 2014, pp. 1049-1066.
- [5] *The progression of atherosclerosis.* Available: https://en.wikipedia.org/wiki/Atherosclerosis#/media/File:Endo_dysfunction_Athero.PNG
- [6] C. G. Caro, J. M. Fitz-Gerald, R. C. Schroter, M. J. Lighthill, and M. G. P. Stoker, "Atheroma and arterial wall shear - Observation, correlation and proposal of a shear dependent mass transfer mechanism for atherogenesis," vol. 177, no. 1046, pp. 109-133, 1971.
- [7] X. He and D. N. Ku, "Pulsatile Flow in the Human Left Coronary Artery Bifurcation: Average Conditions," *Journal of Biomechanical Engineering*, vol. 118, no. 1, pp. 74-82, 1996.
- [8] A. Wahle *et al.*, "Plaque development, vessel curvature, and wall shear stress in coronary arteries assessed by X-ray angiography and intravascular ultrasound," (in eng), *Medical image analysis*, vol. 10, no. 4, pp. 615-631, 2006.
- [9] Ö. Smedby, J. Johansson, J. Mölgaard, A. G. Olsson, G. Walldius, and U. Erikson, "Predilection of Atherosclerosis for the Inner Curvature in the Femoral Artery," vol. 15, no. 7, pp. 912-917, 1995.
- [10] S. J. Head *et al.*, "Mortality after coronary artery bypass grafting versus percutaneous coronary intervention with stenting for coronary artery disease: a pooled analysis of individual patient data," *The Lancet*, vol. 391, no. 10124, pp. 939-948, 2018/03/10/ 2018.
- [11] C. Chen *et al.*, "Simulation of blood flow using extended Boltzmann kinetic approach," *Physica A: Statistical Mechanics and its Applications*, vol. 362, no. 1, pp. 174-181, 2006/03/15/ 2006.
- [12] J. Iqbal, J. Gunn, and P. W. Serruys, "Coronary stents: historical development, current status and future directions," *British Medical Bulletin*, vol. 106, no. 1, pp. 193-211, 2013.
- [13] T. Schmidt and J. D. Abbott, "Coronary Stents: History, Design, and Construction," (in eng), *Journal of clinical medicine*, vol. 7, no. 6, p. 126, 2018.
- [14] *A coronary stent placed by percutaneous coronary intervention.* Available: https://en.wikipedia.org/wiki/Percutaneous_coronary_intervention#/media/File:Blausen_0034_Angioplasty_Stent_01.png
- [15] V. Dehlaghi, M. T. Shadpoor, and S. Najarian, "Analysis of wall shear stress in stented coronary artery using 3D computational fluid dynamics modeling," *Journal of Materials Processing Technology*, vol. 197, no. 1, pp. 174-181, 2008/02/01/ 2008.
- [16] Y. S. Chatzizisis, A. U. Coskun, M. Jonas, E. R. Edelman, C. L. Feldman, and P. H. Stone, "Role of Endothelial Shear Stress in the Natural History of Coronary Atherosclerosis and Vascular Remodeling: Molecular, Cellular, and Vascular Behavior," *Journal of the American College of Cardiology*, vol. 49, no. 25, pp. 2379-2393, 2007/06/26/ 2007.
- [17] K. S. Cunningham and A. I. Gotlieb, "The role of shear stress in the pathogenesis of atherosclerosis," *Laboratory Investigation*, Mini Review vol. 85, p. 9, 11/29/online 2004.
- [18] Z. Sun and Y. Cao, "Multislice CT angiography assessment of left coronary artery: Correlation between bifurcation angle and dimensions and development of coronary artery disease," *European Journal of Radiology*, vol. 79, no. 2, pp. e90-e95, 2011/08/01/ 2011.

- [19] T. Chaichana, Z. Sun, and J. Jewkes, "Computation of hemodynamics in the left coronary artery with variable angulations," *Journal of Biomechanics*, vol. 44, no. 10, pp. 1869-1878, 2011/07/07/ 2011.
- [20] M. Malvè *et al.*, "Tortuosity of Coronary Bifurcation as a Potential Local Risk Factor for Atherosclerosis: CFD Steady State Study Based on In Vivo Dynamic CT Measurements," *Annals of Biomedical Engineering*, vol. 43, no. 1, pp. 82-93, 2015/01/01 2015.
- [21] W. R. Dean, "XVI. Note on the motion of fluid in a curved pipe," *The London, Edinburgh, and Dublin Philosophical Magazine and Journal of Science*, vol. 4, no. 20, pp. 208-223, 1927.
- [22] C. G. Caro, T. Pedley, R. Schroter, and W. Seed, *The mechanics of the circulation*. Cambridge University Press, 2012.
- [23] I. V. Pivkin, P. D. Richardson, D. H. Laidlaw, and G. E. Karniadakis, "Combined effects of pulsatile flow and dynamic curvature on wall shear stress in a coronary artery bifurcation model," *Journal of Biomechanics*, vol. 38, no. 6, pp. 1283-1290, 2005/06/01/ 2005.
- [24] M. Prosi, K. Perktold, Z. Ding, and M. H. Friedman, "Influence of curvature dynamics on pulsatile coronary artery flow in a realistic bifurcation model," *Journal of Biomechanics*, vol. 37, no. 11, pp. 1767-1775, 2004/11/01/ 2004.
- [25] M. F. Rabbi, F. S. Laboni, and M. T. Arafat, "Computational analysis of the coronary artery hemodynamics with different anatomical variations," *Informatics in Medicine Unlocked*, vol. 19, p. 100314, 2020/01/01/ 2020.
- [26] J. Chen and X.-Y. Lu, "Numerical investigation of the non-Newtonian pulsatile blood flow in a bifurcation model with a non-planar branch," *Journal of Biomechanics*, vol. 39, no. 5, pp. 818-832, 2006/01/01/ 2006.
- [27] Y. Papaharilaou, D. J. Doorly, and S. J. Sherwin, "The influence of out-of-plane geometry on pulsatile flow within a distal end-to-side anastomosis," *Journal of Biomechanics*, vol. 35, no. 9, pp. 1225-1239, 2002/09/01/ 2002.
- [28] A. K. Qiao, X. L. Guo, S. G. Wu, Y. J. Zeng, and X. H. Xu, "Numerical study of nonlinear pulsatile flow in S-shaped curved arteries," *Medical Engineering & Physics*, vol. 26, no. 7, pp. 545-552, 2004/09/01/ 2004.
- [29] S. J. Sherwin *et al.*, "The Influence of Out-of-Plane Geometry on the Flow Within a Distal End-to-Side Anastomosis," *Journal of Biomechanical Engineering*, vol. 122, no. 1, pp. 86-95, 1999.
- [30] P. S. Douglas, J. Fiolkoski, B. Berko, and N. Reichek, "Echocardiographic visualization of coronary artery anatomy in the adult," *Journal of the American College of Cardiology*, vol. 11, no. 3, pp. 565-571, 1988/03/01/ 1988.
- [31] *Central line*. Available: <http://www.vmtk.org/tutorials/Centerlines.html>
- [32] T. J. Gundert, S. C. Shadden, A. R. Williams, B.-K. Koo, J. A. Feinstein, and J. F. LaDisa, "A Rapid and Computationally Inexpensive Method to Virtually Implant Current and Next-Generation Stents into Subject-Specific Computational Fluid Dynamics Models," *Annals of Biomedical Engineering*, vol. 39, no. 5, pp. 1423-1437, 2011/05/01 2011.
- [33] S. Beier *et al.*, "Impact of bifurcation angle and other anatomical characteristics on blood flow – A computational study of non-stented and stented coronary arteries," *Journal of Biomechanics*, vol. 49, no. 9, pp. 1570-1582, 2016/06/14/ 2016.
- [34] E. S. Weydahl and J. E. Moore, "Dynamic curvature strongly affects wall shear rates in a coronary artery bifurcation model," *Journal of Biomechanics*, vol. 34, no. 9, pp. 1189-1196, 2001/09/01/ 2001.

Appendix

This work will be presented at the international Australasian Fluid Mechanics conference in December 2020

22nd Australasian Fluid Mechanics Conference AFMC2020
Brisbane, Australia, 6-10 December 2020
DOI: 10.4266/afmc.2020.2022

Impact of Curvature, Bifurcation and Stenting on Secondary Flow in Idealised and Realistic Coronary Arteries

C. Shen¹, T. Camm², R. Gharleghi¹ and S. Beier¹

¹School of Mechanical and Manufacturing Engineering
University of New South Wales, Sydney NSW 2052, Australia

Abstract

Blood flow in healthy coronary arteries is laminar and may have secondary flow generated by vessel curvature, especially where bifurcations are present. Secondary flow impacts local time-averaged wall shear stress (TAWSS), which in turn may be associated with risk of developing atherosclerosis. The objective of this study is to generate insights into the effect of curved small-scale vessels with and without stents on secondary flow profiles and resulting TAWSS effects. Both ideal cylindrical and ideal bifurcated and patient-specific bifurcated vessels were simulated using computational fluid dynamics (CFD). The results showed that presence of vessel curvature generates Dean-like flow in all configurations, leading to the development of two pairs of Dean vortices in each of the daughter branches in the case of bifurcated vessels, and additional flow structures in the region around stents that affect the Dean vortex pair. The influence of curvature on bifurcated vessels is significant, which leads to the flow type asymmetry of the Dean-like flow. The influence of curvature increases with magnitude and distance from the bifurcation divider. The secondary flow structures in regions of curvature result in low TAWSS regions promoting plaque deposition. The presence of stents can disrupt vortices in the daughter branches as well as stented configuration. Overall, this new knowledge contributes to a better understanding of the effect of curved geometry on flow patterns and their effects on local TAWSS.

Keywords

Coronary artery bifurcation, stenting, secondary flow, vortices, dynamics, curvature, haemodynamic, wall shear stress

Introduction

Blood flow patterns have been proven to influence the progression of coronary artery disease. Regions of bifurcation and strong curvature develop Dean-like secondary flow and are prone to atherosclerotic development. Dean first investigated vessel curvature and its effect on flow dynamics in pipe [1], in which secondary flow moved from the outer to the inner surface in the middle of a curved pipe, which has been studied in coronary arteries as well [2]. In bifurcated vessels, the velocity shifts towards the divider [3] and the Dean-like flow loses its symmetry due to the presence of the side branch [4], with the bifurcation dominating the flow velocity structure in the distal daughter branches [5]. The curvature of the artery was found to have a negligible influence on the flow velocity initially increasing as it moves downstream, with distance to the bifurcation region [6]. Studies have also reported that the curvature leads to asymmetric velocity reversals and a strong vortex gradually dominating the secondary flow field in the daughter branches [7, 8]. Additionally, the rheological properties of blood also influenced the local haemodynamics. It was found that the Newtonian fluid was more sensitive to the vessel structure such as curvature, while non-Newtonian blood led to less velocity fluctuation and negligible rotation of flow

velocity profiles [7]. Previous work has been mainly using idealised models [9, 10]. There has been no previous investigations on the effects of curvature, bifurcation and the presence of stents to compare their effects. Further, there is currently no clear understanding of the shape of Dean-like flow and its direction in relation to curvature in a bifurcation. Here, the side branch and curvature were judged separately as a potential cause of velocity profile distortion. The influence of the presence of stents on secondary flow is an important factor in post-surgical care and there has been little work done on this aspect in the context of DNS development and research. Therefore, here the influence of curvature, bifurcation, and stents on the secondary flow in vessels is modelled using an ideal cylinder and idealised bifurcation models with a range of curvatures ($0^\circ, 45^\circ, 75^\circ, 105^\circ$). In addition, a patient-specific bifurcation and a stented bifurcation model is also analysed to study their implications on real-life scenarios. Overall, this work may increase understanding of secondary flow fields in bifurcated coronaries associated with atherosclerosis development.

Methods

Modelling of Vessel Geometries

In this work, ideal cylinder models, ideal bifurcation models, and a patient-specific model (Figure 1) are simulated to investigate the effects of curvature, bifurcation and presence of a stent on local flow development.

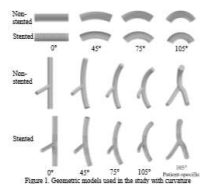


Figure 1: Schematic diagrams used in the study. (a) Ideal cylinder models, (b) ideal bifurcation models, and (c) patient-specific model. The curvature of the ideal bifurcation model is defined as an arc (Figure 2a) with the diameter and length of curved segment being 8 mm and 10 mm, respectively. These are estimated using the equation: $k = \frac{1}{R} = \frac{1}{R \sin \theta}$, $\theta = \frac{\pi}{2} (k = \text{curvature } R = \frac{1}{k})$

radius R is central angle θ , with a central angle defining the curvature. Since the curved segment is of fixed length, a larger central angle represents a larger curvature. Thus, the ideal models are set to $0^\circ, 45^\circ, 75^\circ$ and 105° curvature magnitudes. To obtain a fully developed flow profile when the flow enters the curved segment, a 15-mm-long entrance length is set following the inlet. The ideal bifurcation is defined to wrap around a sphere which mimics the heart (Figure 2b). The curvature of the main branch (MB) and side branch (SB) are determined by the central angle in the same manner as the ideal cylinder model. Parameters of the ideal bifurcation model are determined based off a patient-specific bifurcation geometry with the length and diameter of MB and SB are 7.5 mm and 11 mm, and the diameters, 2.8 mm, and 2 mm, respectively and bifurcation angle of 60° . The patient-specific bifurcation model is subsequently used to compare haemodynamics. For the stented geometry, a stent with a rectangular cross-section is implanted on them to compare the influence of stenting on secondary flow.

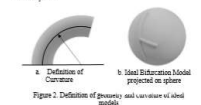


Figure 2: Definition of geometry and curvature of ideal models.

Computational Method

Numerical simulations are performed using the commercially available Navier-Stokes solver ANSYS CFX (Canonburg, PA). Blood is modelled using a laminar, Carreau-Yasuda non-Newtonian model [11]. The simulations are initially run as steady state, before being used as initiation for a transient solution to damp initial effects. The fourth cycle is used for the analysis of the simulation. Hemodynamic parameters such as the time-averaged wall shear stress (TAWSS) and the velocity distributions are extracted from each of the simulations for comparison. These geometries are generated using AutoCAD Inventor (San Rafael, CA), which are then projected [12] onto the artery presentation using a Boolean approach to define the fluid volume to be modelled for all stented configurations.

Results

Flow analysis

Cross-sections located at the centre of curvature for the ideal cylinders and on locations for the ideal and patient-specific bifurcations are chosen along the geometry to analyse and compare flow behaviour (Figure 3). The velocity streamlines are plotted at all the chosen locations for each configuration along with TAWSS distributions. The vorticity

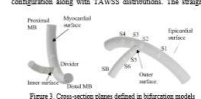


Figure 3: Cross-section planes defined in bifurcation model.

cylinder shows no secondary flow as expected, whereas the equivalent curved models show significant secondary flow vortices (Figure 4).

The flow in the cylindrical models, due to the changed vessel shape, moves from epistemic to the myocardial surface along

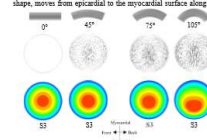


Figure 4: Dean-like flow in ideal cylinder models.

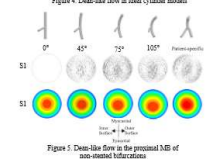


Figure 5: Dean-like flow in the proximal MB of non-stented bifurcations.

the inner side of the vessel wall and returns inside the vessel. A pair of symmetric Dean vortices are formed on either side of the curvature normal. When the curvature is increased, the flow centre shifts to the epistemic surface and the velocity profile turns to an apparent crescent shape. In the proximal main branch of the non-stented bifurcation model, Dean-like flow is observed with the velocity profile showing a similar characteristic as that in ideal cylinder models (Figure 5). A similar development of flow vortices is seen in the side branch, which is more pronounced in the patient-specific model with the vortices developing in an angular orientation before the divider (i.e. in the proximal main branch Figure 5). After the flow splits due to the divider, flow separation and vortex formation takes place in addition to the secondary flow effects (Figure 6).

Figures 7 and 8 fully developed Dean-like flows are shown to occur at several locations in the main branch and side branches of the bifurcation. In the first Dean-like flow (S1, S5), the flow moves from the inner to the outer surface and returns along the diameter. But the second Dean-like flow (S4, S6) shows an opposite orientation. In the ideal bifurcation model

(non-curved), the pair of Dean-like flow vortices are symmetrical in the two daughter branches. In curved models, the vortices in daughter branches appear asymmetric. The rotational magnitude of the first Dean-like flow (S1, S5) is relatively small, but the flow symmetry is apparent. The vortices near the epistemic surface increase in size while the size near myocardial surface decreases, in both daughter branches. In the 105° curved model, the second Dean-like flow vortices (S4) in proximal MB are symmetrically present on the either side of the curvature normal in both daughter branches. Additionally, there is vortex dissipation in the side branches and secondary flow structures (L-type and W-type) composed

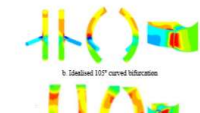


Figure 6: TAWSS distributions in stented bifurcation model.

Figure 7: TAWSS distributions in idealised 0° and 105° curved and patient-specific bifurcation models.

TAWSS contour plots are shown in Figure 9, and 10, for the cylindrical and bifurcation models, respectively. Curvature in the branches directly affected TAWSS distributions values at the inner and outer wall regions in both the cylindrical and bifurcation models. The inherent curvature of the proximal main branch and side branches in a patient-specific bifurcation model and secondary flow vortices form at all locations where there is a significant curving of the artery thereby predisposing the site to adversely low TAWSS and hence plaque deposition.

Stented Configurations

Stents in the MB were added to the previously simulated cylinder and bifurcation. L-type and W-type flow structures in the branches were seen in addition to the Dean-type vortices (Figure 11). The L-type and W-type vortices are formed due to disruption of the Dean-type vortices with the magnitude of curvature.

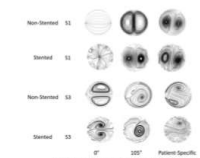


Figure 8: Dean-like flow in SB of non-stented bifurcations.

Figure 9: Dean-like flow in the cross-sectional flow structures at S1 and S5 as compared to S4.

Wall Shear Stress Distribution

Figure 9: TAWSS distributions in ideal cylindrical model.

Figure 10: TAWSS distributions in ideal cylindrical model.

Figure 11: Secondary flow structures in the MB of stented models.

There is additionally an effect on TAWSS with large areas of low TAWSS forming around the area where the stents are placed (Figure 12). The area surrounding the stents shows the flow to develop the L-type and W-type vortices downstream as shown in Figure 11. The area around the stents have a lower TAWSS of 0.1 Pa as compared to 0.50 Pa in unobstructed bifurcations.

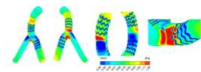


Figure 12: TAWSS distributions in stented bifurcation model.

Discussion

An understanding of the effect of curvature, bifurcation and stenting on coronary arteries is essential to understanding coronary haemodynamics. Curvature is known to be the primary factor in secondary flow development [1, 6]. Our simulations involving both idealised and patient-specific bifurcation configurations show significant influence of curvature in generating Dean-like flow in the proximal MB and a pair of Dean vortices in each daughter branch (SB) for a range of curvatures investigated. Flow in the unobstructed proximal MB is mainly influenced by curvature and can be considered as being equivalent to a cylinder as it shows similar secondary flow structures as well as TAWSS distributions. The identified vortices develop and loss of symmetry in bifurcations agree with previous findings in addition to the secondary flow structures in the SB involving L-type and W-type vortices structures as seen by Balas and Pleskac [13]. The flow vortices in each case of curved arteries tend to move to the epistemic surface of the curvature, and Dean-like flow tends towards becoming more symmetric. The vortex near epistemic surface tends to dominate the secondary flow field. With the increase of curvature, the influence of curvature in the Dean-like flow generated by bifurcation structure will increase, which has been directly proved by a previous study [13]. Furthermore, the increased curvature will gradually control the Dean-like flow with the increase of distance from divider in the distal MB. Although the influence of curvature is significant according to the 3D velocity vector (Figure 1a), the bifurcation structure determines the typical velocity distribution in daughter branches near the divider. Following on from Weidali et al. [2], high shear rates occur on the inner surface while low shear rates on the outer surface leading to high and low TAWSS regions, respectively. The low TAWSS regions promote atherosclerotic plaque deposition.

The influence of stents is significant on Dean-like flow in ideal cylinder and proximal MB in bifurcations. Additionally, in distal MB, the presence of stents changes the Dean-like flow structures. Following from [21], there is a significant flow breakdown and sub-structures of the flow such as L-type and W-type vortices are formed. There are in addition to the vortices formed around the main stents as shown in Figure 11, for the cross-section S3. These flow structures warrant future work on the flow development downstream of stents. The significant effect of placing stents in the bifurcation in the development of a low TAWSS regions making it predisposed to atherosclerotic plaque deposition and this may present an important clinical insight.

Conclusions

The effect of curvature and bifurcations on the development of secondary flow in different bifurcation configurations are investigated with and without stents. We demonstrated the significant effect of curvature on secondary flow vortices and then TAWSS in these regions. The presence of stents has a significant effect on the developed flow field in all models. Dean's vortices generated due to the vessel geometry are an important fluid dynamic effect that need to be considered in the

context of coronary artery disease with a direct relevance for the understanding of atherosclerotic plaque development.

Acknowledgments

This work was undertaken with the assistance of resources from the National Computational Infrastructure (NCI), an NCIIS enabled facility supported by the Australian Government.

References

- [1] Dean W.R. (1927). Vortex lines on the motion of fluid in a curved pipe. *The London, Edinburgh, and Dublin Philosophical Magazine and Journal of Science*, 4 (20), 218-223.
- [2] Weidali H.E., and Moore J.E. (2001). Dynamic curvature strongly affects wall shear rates in coronary artery bifurcation model. *Journal of Biomechanics*, 34(9), 1189-1196.
- [3] Carr C.O., Peller T., Schuster K., and Seed W. (2012). The mechanics of the circulation. Cambridge University Press.
- [4] Pleskac, I. V., Richardson, P. D., Laidlaw, D. H., and Karimkhanlou, O. R. (2005). Combined effects of pulsatile flow and dynamic curvature on wall shear stress in a coronary artery bifurcation model. *Journal of Biomechanics*, 38(9), 1283-1290.
- [5] Pleskac, I. V., Richardson, P. D., Laidlaw, D. H., and Karimkhanlou, O. R. (2005). Combined effects of pulsatile flow and dynamic curvature on wall shear stress in a coronary artery bifurcation model. *Journal of Biomechanics*, 38(9), 1283-1290.
- [6] Pleskac, I. V., Richardson, P. D., Laidlaw, D. H., and Karimkhanlou, O. R. (2005). Combined effects of pulsatile flow and dynamic curvature on wall shear stress in a coronary artery bifurcation model. *Journal of Biomechanics*, 38(9), 1283-1290.
- [7] Chen, L., and Li, X. Y. (2008). Numerical investigation of the non-Newtonian pulsatile blood flow in a bifurcation model with a non-planar branch. *Journal of Biomechanics*, 41(5), 815-822.
- [8] Pleskac, I. V., Dean, D. J., and Shew, S. S. (2004). The influence of out-of-plane geometry on pulsatile flow within a distal and to-side anastomosis. *Journal of Biomechanics*, 37(9), 1225-1239.
- [9] Qian, A. K., Gao, X. L., Wu, S. B., Zeng, Y. J., and Ma, M. R. (2004). Physical study of nonlinear pulsatile flow in S-shaped curved arteries. *Medical engineering & physics*, 26(7), 544-552.
- [10] Shew, S. J., Shah, O., Dorsey, D. J., Patel, J., Papadimitrakaki, F., Wilson, J., Carr C.O., and D'Amato, C. L. (2000). The influence of out-of-plane geometry on the flow within a distal and to-side anastomosis. *J. Biomech. Eng.*, 122(1), 64-70.
- [11] Carreau, Y. C., Dussan-Velez, F., Violette, M., Cass, J., Nappi, S., Meunier-Guillet, P., Yung, A., and Carr C.O. (2016). Impact of bifurcation angle and side anastomosis characteristics on blood flow-A computational study of non-stented and stented coronary arteries. *Journal of Biomechanics*, 49(9), 1370-1381.
- [12] Omid, T. J., Shadloo, S. C., Vahdani, A. R., Koo, B. K., Feustel, J. A., and Laidlaw, J. F. (2011). A rapid and computationally intensive method to virtually implant current and next-generation stents into subject-specific computational fluid dynamics models. *Annals of biomedical engineering*, 39(7), 1423-1437.
- [13] Balas, K. V., and Pleskac, M. W. (2011). Secondary flow morphologies due to model stent-induced perturbations in a 180° curved tube during systolic distension. *Experiment in fluids*, 54(3), 1493.